Published March 15, 2010

Inner centromere formation requires hMis14, a trident kinetochore protein that specifically recruits HP1 to human chromosomes

Tomomi Kiyomitsu,[1] Osamu Iwasaki,[2] Chikashi Obuse,[2] and Mitsuhiro Yanagida[1]

[1]Core Research for Evolutional Science and Technology Research Program, Japan Science and Technology Corporation, Department of Gene Mechanisms, Graduate School of Biostudies, Kyoto University, Sakyo-ku, Kyoto 606-8501, Japan
[2]Faculty of Advanced Life Science, Hokkaido University, Kita-ku, Sapporo 001-0021, Japan

Centromeric DNA forms two structures on the mitotic chromosome: the kinetochore, which interacts with kinetochore microtubules, and the inner centromere, which connects sister kinetochores. The assembly of the inner centromere is poorly understood. In this study, we show that the human Mis14 (hMis14; also called hNsl1 and DC8) subunit of the hetero-tetrameric hMis12 complex is involved in inner centromere architecture through a direct interaction with HP1 (heterochromatin protein 1), mediated via a PXVXL motif and a chromoshadow domain. We present evidence that the mitotic function of hMis14 and HP1 requires their functional association at interphase. Alterations in the hMis14 interaction with HP1 disrupt the inner centromere, characterized by the absence of hSgo1 (Shugoshin-like 1) and aurora B. The assembly of HP1 in the inner centromere and the localization of hMis14 at the kinetochore are mutually dependent in human chromosomes. hMis14, which contains a tripartite-binding domain for HP1 and two other kinetochore proteins, hMis13 and blinkin, is a cornerstone for the assembly of the inner centromere and kinetochore.

Introduction

Faithful chromosome segregation during mitosis requires a specific region of the chromosome called the kinetochore. The kinetochore associates with spindle assembly checkpoint proteins and kinetochore microtubules during mitosis (Rieder and Salmon, 1998; Cleveland et al., 2003; Amor et al., 2004; Chan et al., 2005; Musacchio and Salmon, 2007). The principal constricted region of vertebrate metaphase chromosomes consists of bidirectionally located sister kinetochores, which are connected by a structure called the inner centromere. The inner centromere is a heterochromatic domain that is a focus for cohesins and regulatory proteins such as aurora B passenger protein kinase. The inner kinetochore is a region of distinct chromatin composition at the interface with the inner centromere, whereas the outer kinetochore is the site of microtubule binding. The kinetochore and the inner centromere contain many proteins, most of which differ between these two structures. For example, proteins CENP-A and -C are present in the inner kinetochore, whereas CENP-B, cohesin, and HP1 (heterochromatin protein 1) are present in the inner centromere (Cooke et al., 1990; Saitoh et al., 1992; Sullivan et al., 1994; Hoque and Ishikawa, 2001). However, centromeric DNAs specific for the kinetochore or inner centromere have not been reported. Therefore, the same DNA sequence may constitute the kinetochore and the inner centromere. The great majority of vertebrate centromeric DNAs are known to contain the highly repetitive satellite DNA sequences (Schueler and Sullivan, 2006). Little is known about the order of events for inner centromere and kinetochore assembly onto the centromeric DNAs to form the metaphase chromosome.

Proteins bound to the inner centromere have variable functions. CENP-B (Earnshaw and Rothfield, 1985) binds to the 17-bp CENP-B box on α-satellite DNA (Masumoto et al., 1989) and is needed for de novo centromere formation (Okada

T. Kiyomitsu and O. Iwasaki contributed equally to this paper.

Correspondence to Mitsuhiro Yanagida: yanagida@kozo.lif.kyoto-u.ac.jp

O. Iwasaki's present address is The Wistar Institute, Philadelphia, PA 19104.

Abbreviations used in this paper: AS, asynchronous; CD, chromodomain; CSD, chromoshadow domain; WT, wild type; Y2H, yeast two-hybrid.

Supplemental Material can be found at:
http://jcb.rupress.org/content/suppl/2010/03/15/jcb.200908096.DC1.html

The Rockefeller University Press $30.00
J. Cell Biol. Vol. 188 No. 6 791–807
www.jcb.org/cgi/doi/10.1083/jcb.200908096

Published March 15, 2010

et al., 2007). Cohesin holds sister chromatids together (Hauf et al., 2001), whereas Shugoshin and protein phosphatase 2A protect cohesin (Kitajima et al., 2006). The heterotetrameric aurora B kinase (chromosome passenger complex) has multiple functions ranging from chromosome–microtubule interactions to sister chromatid cohesion and cytokinesis (Ruchaud et al., 2007). Pericentric heterochromatin contains Lys9-methylated histone H3, which provides the characteristic features of heterochromatin. Indeed, HP1 is strongly enriched at the inner centromere (Sugimoto et al., 2001). HP1 recognizes Lys9-methylated histone H3, which specifically exists in heterochromatin, and recruits several regulatory proteins (Grewal and Jia, 2007). HP1 contains both a chromodomain (CD) and a chromoshadow domain (CSD; Nielsen et al., 2002; Thiru et al., 2004; Koch et al., 2008); the CD recognizes Lys9-methylated histone H3, whereas the CSD interacts with PXVXL-containing, HP1-binding proteins. Histone methyltransferase Suv39h, which methylates histone H3 Lys9, is required for the recruitment of HP1 at the inner centromere.

The kinetochore has a highly complex structure and contains a large number of evolutionarily conserved proteins, in contrast to centromeric DNAs, which are highly divergent in sequence and length (Yanagida, 2005). The kinetochore is assembled on nucleosomes, which contain a kinetochore-specific histone H3 variant CENP-A. CENP-A is conserved among eukaryotes and is required for the assembly of most other kinetochore proteins, although CENP-A–containing nucleosomes do not appear to be sufficient for full kinetochore assembly in vertebrates (Howman et al., 2000; Van Hooser et al., 2001; Goshima et al., 2003; Liu et al., 2006). Mis12, a member of another evolutionarily conserved kinetochore protein family, is also required for the formation of a functional kinetochore (Goshima et al., 1999, 2003). Studies involving fission yeast genetics and RNAi studies in mammalian cells suggest that the recruitment pathways for Mis12 and CENP-A are independent, although they localize to almost the same regions (Takahashi et al., 2000; Goshima et al., 2003; Hayashi et al., 2004; Fujita et al., 2007). Liu et al. (2006) report that human Mis12 (hMis12) localization may be specified by CENP-A in human cells. The hMis12 complex consists of four subunits: hMis12, hMis13/c20orf172/hDsn1, hMis14/DC8/hNsl1, and hNnf1/PMF1 (Cheeseman et al., 2004; Obuse et al., 2004; Kline et al., 2006; Kiyomitsu et al., 2007). During mitosis, the hMis12 complex assembles the kinetochore protein blinkin (also called hSpc105, hKNL1, CASC5, and D40) and checkpoint proteins Bub1 and BubR1 at the kinetochores, and this step is essential for chromosome alignment and the mitotic checkpoint (Kiyomitsu et al., 2007).

Although our understanding of the organization of the inner centromere and kinetochore of eukaryotic cells is rapidly increasing, there is still little information about how these two structures are connected. The boundary between the kinetochore and the inner centromere must be formed and maintained by specific regulatory mechanisms, as the protein components of these two structures are so distinct. In this study, we investigated how the inner centromere and the kinetochore functionally interact to form a connected structure at the molecular level in human cells. We previously reported that a functional link might exist between the inner centromere and the kinetochore because human kinetochore protein hMis12 was coimmunoprecipitated with HP1-α and -γ and kinetochore proteins blinkin and Zwint-1 (Obuse et al., 2004; Kiyomitsu et al., 2007). Moreover, the simultaneous depletion of HP1-α and -γ by double RNAi abolished centromeric localization of hMis12 and hMis14/DC8 in interphase (Obuse et al., 2004). Therefore, we examined which kinetochore protein actually makes direct contact with HP1.

Results

Coimmunoprecipitation of hMis12 with the HP1-α CSD fragment

The N-terminal CD, the central hinge and the C-terminal CSD of human HP1-α are schematized in Fig. 1 A (top). By expressing Flag-tagged CD (aa 1–67) or CSD (aa 110–191) fragments of HP1-α in human 293 cells, followed by immunoprecipitation using anti-Flag antibodies, we determined which domain of HP1-α coimmunoprecipitated with hMis12 and hMis13 proteins. Immunoblot data showed that the CSD but not the CD coprecipitated with hMis12, hMis13, and HP1-γ (Fig. 1 A, bottom). HP1-α and -γ are known to interact with each other through the CSD (Brasher et al., 2000). The addition or deletion of a hinge domain to CD or CSD showed no effect on the coimmunoprecipitation of hMis12 and HP1 (Fig. S1 A).

Yeast two-hybrid (Y2H) interaction of hMis14 with HP1 CSD

To determine which subunit of the hMis12 complex directly interacts with CSD, a pairwise Y2H screen was performed between the CSD of HP1-α, -β, or -γ and one of the four subunits of the hMis12 complex. Only hMis14 was found to be positive in the Y2H interaction with the CSD of HP1-α, -β, or -γ (Fig. 1 B). Consistently, four substitution mutants of CSD, I165E, T173D, T173K, and W174A, which were defective in dimer formation and/or hydrophobic pocket formation (Brasher et al., 2000; Thiru et al., 2004), failed to interact with hMis14 (Fig. 1 C and Fig. S1 B). hMis14 might recognize and directly interact with the hydrophobic pocket of the dimeric CSD of HP1.

A short region of hMis14 interacts with HP1 CSD

To determine which region of hMis14 interacted with HP1-α, we made various hMis14 mutants, which were subsequently tested in the Y2H assay. The amino acid sequence of hMis14 contains two predicted CSD-binding sequences, ^{5}PELVV and ^{209}PVIHL (consensus [P/L]XVX[M/L/V]; Smothers and Henikoff, 2000; Thiru et al., 2004). Construction of substitution mutants and subsequent Y2H established that only ^{209}PVIHL was relevant for the Y2H interaction with HP1. The substitution mutant m1E (in which Leu7 was replaced with Glu in the full-length hMis14) retained full ability to interact with HP1-α, whereas the substitution mutant m2E (in which Ile211 and Leu213 were replaced with Glu in the full-length hMis14) was completely defective for interaction with HP1-α (Fig. 1 D). Moreover, the short

Published March 15, 2010

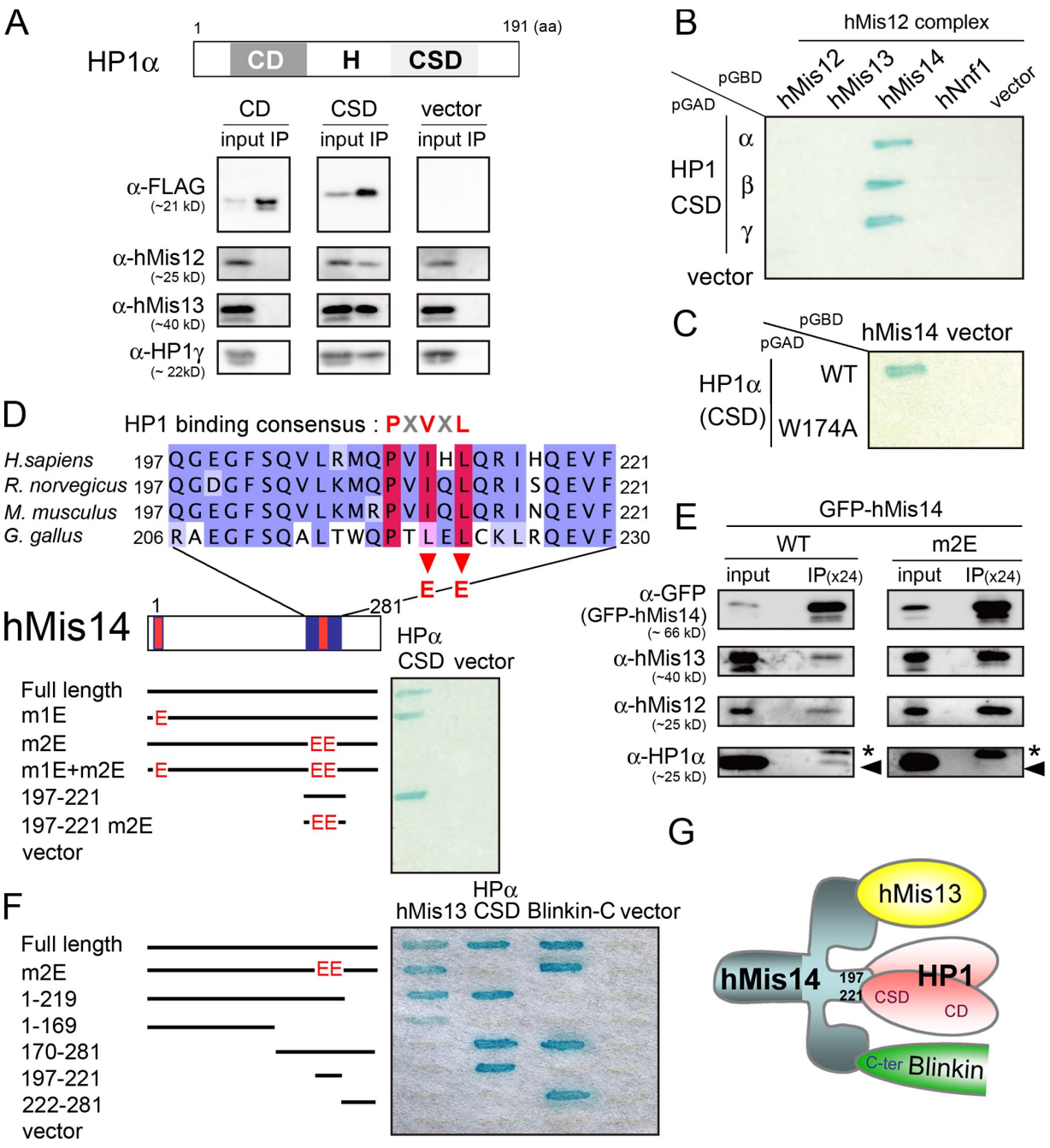

Figure 1. **Direct interaction between hMis14 and HP1 and construction of the hMis14 m2 mutant.** (A) Human 293 cells were transfected with a plasmid that expressed the Flag-tagged CD or CSD of HP1-α. Extracts were prepared 30 h after transfection using the cytoskeleton buffer and subjected to immunoprecipitation. Input and immunoprecipitates (IP) were immunoblotted using the antibodies indicated. Empty vector was transfected as a control. H, hinge. (B) Y2H experiments between the four subunits of the hMis12 complex and the CSD of HP1-α, -β, or -γ. (C) Y2H analysis between hMis14 and an HP1-α CSD mutant. (D) Amino acid sequences of Mis14 family members. Conserved amino acids are boxed in dark purple, and similar amino acids are boxed in light purple. HP1-binding PXVXL motifs are shown in red. Y2H analysis was performed between deletions or substitutions of hMis14 and HP1-α CSD. (E) Immunoprecipitation of GFP-tagged WT and mutant constructs (m2E) of hMis14. Immunoblot was performed using the antibodies indicated. The band position of HP1-α is indicated by the arrowheads. The band indicated by the asterisks is contaminating IgG. (F) Y2H analysis between various deletions and substitutions of hMis14 and hMis13, HP1-α CSD, and the blinkin C-terminal fragment, blinkin-C (aa 1981–2316). (G) A cartoon depicting interactions detected between the hMis12 complex, blinkin, and HP1.

25-aa fragment (197–221) with the ^{209}PVIHL consensus could still retain the ability to interact with HP1-α, whereas the same fragment containing the m2E mutations (I211E and L213E) abolished the interaction with HP1-α. Thus, the 197–221 region of hMis14 with the consensus sequence for HP1 binding was capable of interacting with HP1.

To examine whether the PXVXL-dependent interaction also occurred in human cells, GFP-tagged hMis14 wild-type (WT) and mutant m1E and m2E plasmids were transfected into 293 cells, and the extracts were immunoprecipitated with anti-GFP antibodies. HP1-α was coprecipitated with GFP-hMis14 WT but not with the GFP-hMis14 m2E mutant (Fig. 1 E).

Published March 15, 2010

HP1-α was coprecipitated by the m1E mutant but not by the m1E + m2E mutant (Fig. S1 C). Collectively, the direct interaction between hMis14 and HP1 mediated through the CSD-binding motif may also occur in human cells.

hMis14 binding to hMis13, HP1, and blinkin

The hMis14 m2E mutant that failed to bind to HP1-α was nonetheless coprecipitated with two kinetochore proteins (hMis13 and hMis12) in human cells (Fig. 1 E). This strongly suggests that the ability of hMis14 to interact with these two proteins was independent of HP1-binding activity. hMis13 and hMis14 form a heterodimer that interacts with blinkin (Kiyomitsu et al., 2007). Thus, we dissected the regions of hMis14 that were necessary for its interaction with HP1, hMis13, and blinkin by performing Y2H assays with various truncation mutants of hMis14 and HP1, hMis13, and blinkin proteins (Fig. 1 F). The results indicated that the hMis14 N-terminal region (1–169 aa) and C-terminal region (222–281 aa) were necessary and sufficient for interaction with hMis13 and blinkin, respectively. The hMis14 m2E mutant was able to bind to both hMis13 and blinkin, suggesting that this mutant specifically lacked the ability to interact with HP1-α. The other substitution mutant m2A (in which Ile211 and Leu213 were replaced with Ala in the full-length hMis14) showed the same result as m2E: it did not interact with HP1-α but could interact with hMis13 and blinkin-C (Fig. S1 D). Collectively, hMis14 contains three nonoverlapping regions for binding to hMis13, HP1, or blinkin (Fig. 1 G). The N-terminal region of hMis14 forms a part of the hMis12 complex by directly associating with hMis13 (Kiyomitsu et al., 2007). The short middle region (197–221) of hMis14 is the HP1-binding site, whereas the C-terminal region (221–281) binds to the C terminus of blinkin (blinkin-C).

hMis14 interacts with HP1 during interphase

To examine the interaction between hMis14 and its binding partners during the cell cycle, we generated a HeLa cell line that stably expressed GFP-hMis14 and performed immunoprecipitation of GFP-hMis14 from asynchronous (AS) or nocodazole-arrested mitotic extracts. Both hMis13 and hMis12 coprecipitated with GFP-hMis14 at almost equal levels in AS and nocodazole-arrested extracts, suggesting that the hMis12 complex is stable during the cell cycle. In contrast, HP1-α coprecipitated predominantly in the AS extract (Fig. 2 A). The hMis12-interacting kinetochore proteins blinkin, Bub1, Zwint-1, and Ndc80 were detected by coimmunoprecipitation mainly in nocodazole-arrested extracts. These results indicated that hMis14 alters its binding partners during the cell cycle.

To examine this more rigorously, we did an inverse experiment, using a HeLa cell line that stably expressed GFP–HP1-α. HP1-γ coprecipitated with GFP–HP1-α almost equally in both extracts, but hMis12 and hMis13 coprecipitated predominantly in the AS extract (Fig. 2 B). Blinkin, Bub1, and Ndc80 were not detected in the precipitates, but an intense band of aurora B was detected in GFP–HP1-α immunoprecipitates from mitotic (nocodazole arrested) extracts.

The localization of hMis14 and HP1-α was subsequently examined in interphase cells and on chromosomes in a metaphase spread. HP1-α is known to be enriched at centromeric and heterochromatic regions during interphase and at the inner centromere in the mitotic chromosome (Minc et al., 1999; Sugimoto et al., 2001; Hayakawa et al., 2003). Our results show that the signals of hMis14 and HP1-α overlapped during interphase, whereas their localization was clearly distinct on metaphase spread chromosomes (Fig. 2 C). Collectively, our results show that hMis14 binds to HP1 during interphase but that its binding preference shifts toward binding to blinkin and Ndc80 kinetochore proteins during mitosis. In contrast, HP1 binds to hMis14 during interphase, but it binds to aurora B during mitosis.

Recruitment of HP1-α to the inner centromere requires hMis14

To determine the role of hMis14 in the enrichment of HP1-α at the inner centromere, we performed a functional analysis by knocking down hMis14 using RNAi. 48 h after siRNA infection, the level of hMis14 detected by immunoblot was negligible (Fig. 3 A). During mitosis in hMis14 RNAi cells, the kinetochore signals of hMis14 were abolished, as expected, and extensive misalignment of chromosomes was observed (Fig. 3 A, bottom). During interphase, the dot signals of GFP–HP1-α, which colocalized with CENP-B signals, were reduced after hMis14 RNAi (Fig. 3 B and Fig. S2 A). In the metaphase chromosomes, the signals for GFP–HP1-α were broadly diffused along the chromosomes after hMis14 RNAi (Fig. 3 C, top), whereas the GFP–HP1-α signal was intense at the inner centromeres in control cells (Fig. 3 C, bottom). In hMis14 RNAi, the primary constriction of the metaphase chromosome was lost. Because the inner centromeric CENP-B signals (Fig. 3 C, magenta) were intense and frequently doubled, "sister" inner centromeres could have formed only partly and remained disconnected. However, in the control RNAi cells, the CENP-B signals were mostly single (Fig. S2 [B and C] supports these conclusions), as the inner centromere is complete. Therefore, the recruitment of CENP-B to the inner centromere does not require HP1-α. CENP-B is known to directly bind to a satellite DNA sequence motif that is abundant in human centromeres (Masumoto et al., 1989).

Distinct states of cohesion after RNAi of hSgo1, hMis14, or HP1

The hSgo1 (Shugoshin-like 1) protein, which interacts with HP1-α (Yamagishi et al., 2008), was also not enriched at the inner centromere after hMis14 RNAi (Fig. 3 C). Because the role of hSgo1 in the formation of the inner centromere was unclear, we compared the RNAi phenotypes of hSgo1 with those of hMis14 and HP1. In RNAi-treated cells, spread mitotic chromosomes were stained by an antibody against hSgo1. DNA was counterstained by Hoechst 33342. In hSgo1 RNAi cells, most cells (93%; $n = 100$) showed the complete separation of sister chromatids (Fig. 3 D, second column), as was previously reported (Kitajima et al., 2005), and anti-Sgo1 antibody staining revealed no signal along the chromosome. However, in hMis14 RNAi–treated cells, most chromosomes showed separated but

Published March 15, 2010

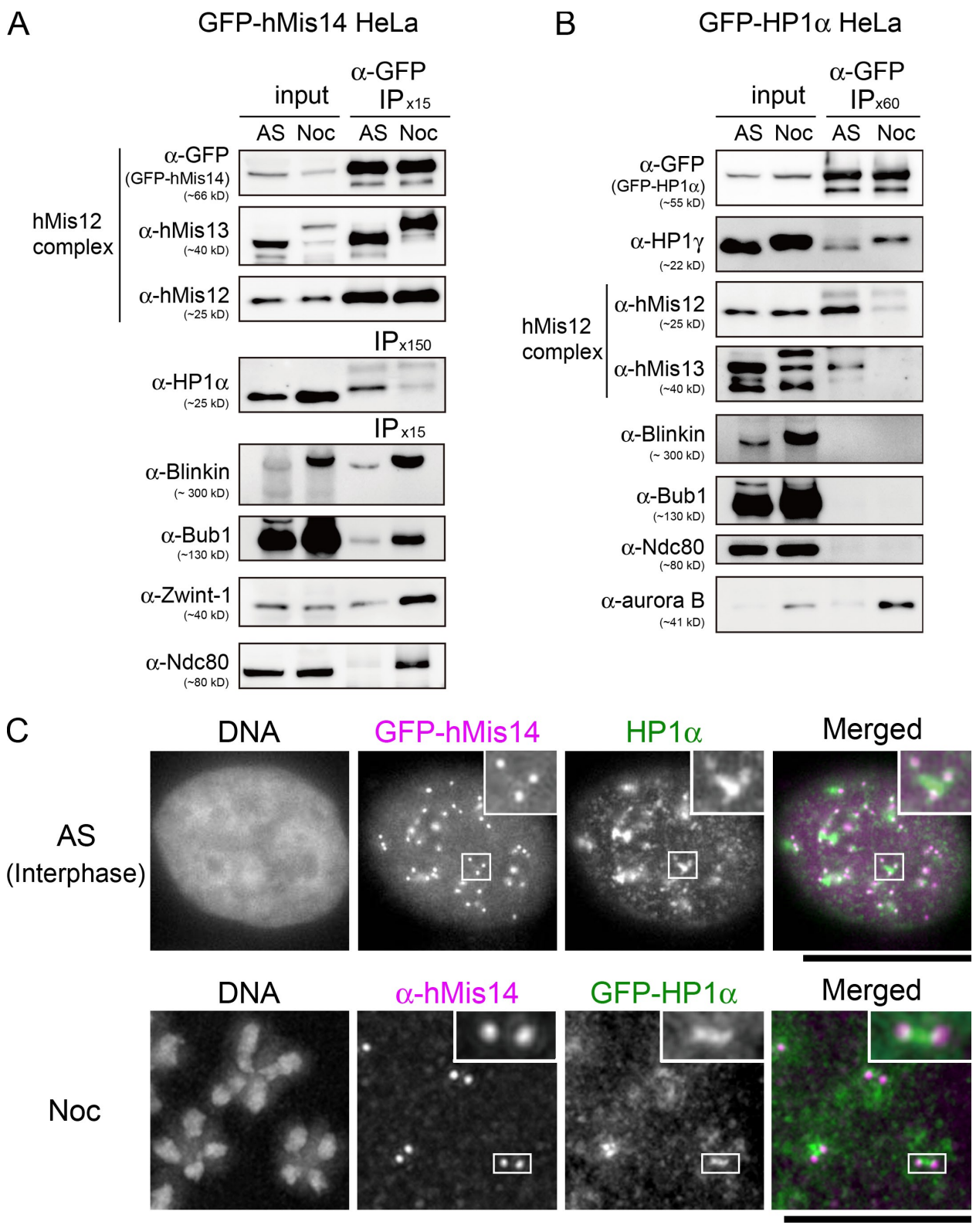

Figure 2. **Interaction between hMis14 and HP1 in interphase.** (A and B) Immunoprecipitation (IP) of GFP-tagged hMis14 (A) and HP1-α (B). Cultures of HeLa cells that stably expressed GFP-tagged hMis14 or HP1-α were used: AS culture is predominantly interphase, and nocodazole-arrested (Noc) culture is mitotically arrested. (C) Interphase HeLa cells that stably expressed GFP-hMis14 were stained with antibodies against HP1-α (top). Metaphase spread chromosomes of HeLa cells stably expressing GFP–HP1-α were stained with anti-hMis14 antibodies (bottom). Cross section images were deconvolved and stacked. Insets show a higher magnification view of the boxed areas. Bars, 10 μm.

Published March 15, 2010

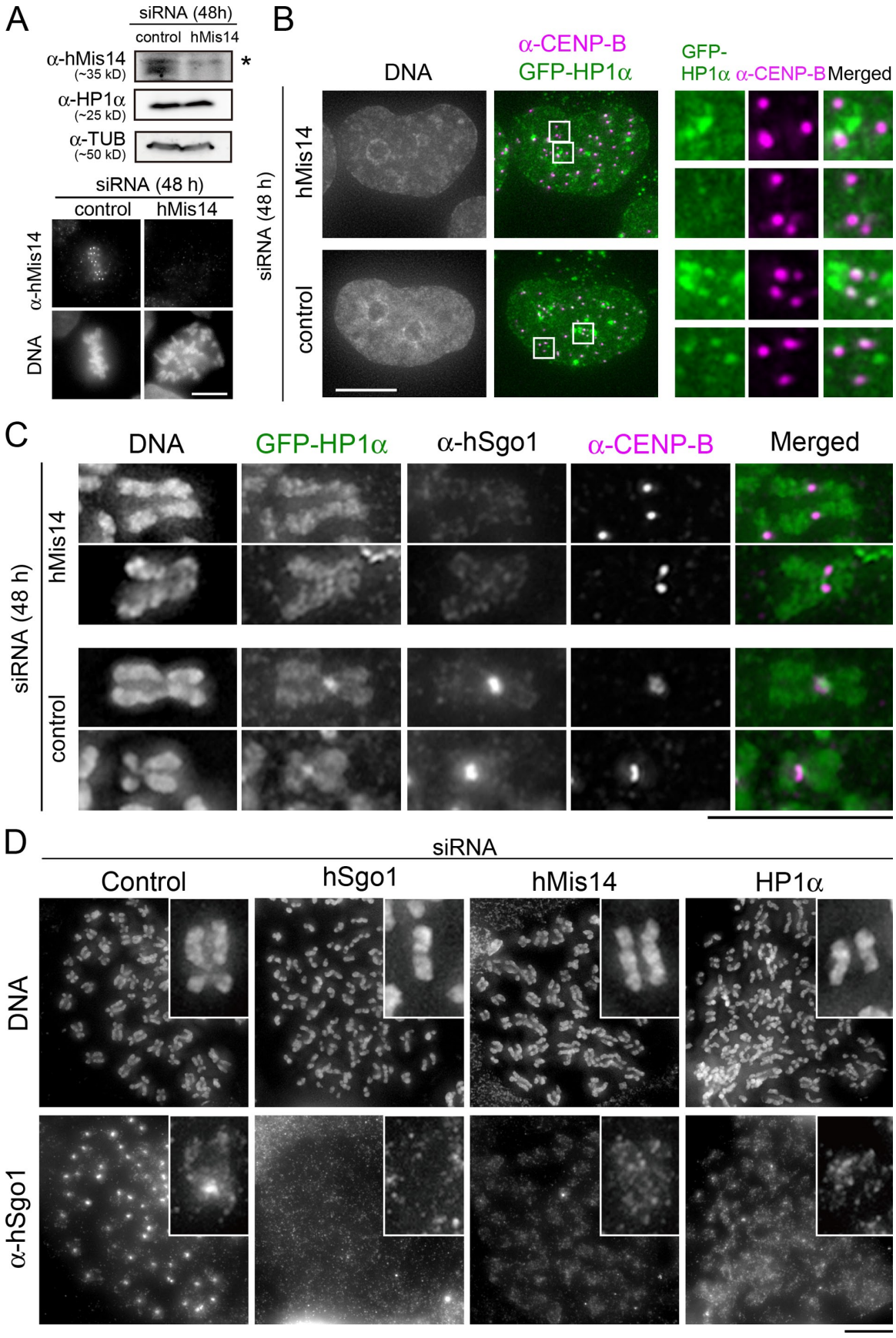

Figure 3. **hMis14-dependent enrichment of GFP–HP1-α at the inner centromere.** (A) Immunoblot of hMis14 after RNAi treatment. The loading control was tubulin (TUB). Bands indicated by the asterisk are proteins that cross react with anti-hMis14 antibodies (top). HeLa cells were fixed and stained with

Published March 15, 2010

still paired sister chromatids (95%; $n = 100$), and anti-hSgo1 antibody dimly stained the arm regions. The primary constriction that would require the normal connection of sister inner centromeres was absent in a significant fraction (36%) of spread chromosomes (Fig. 3 D, third column; compare with first column of control no RNAi). In HP1-α RNAi–treated cells, spread chromosome staining resembled that in hMis14 RNAi cells, namely, 90% of cells ($n = 100$) showed paired chromatids. About 50% of these cells clearly lacked a primary constriction, whereas sister chromatids were partially separated (Fig. 3 D, fourth column). The anti-hSgo1 antibody only weakly stained the arm regions. However, in control RNAi cells, anti-hSgo1 antibody signals were highly enriched at the inner centromere (89%; $n = 100$). Collectively, these results show that arm cohesion and also possibly residual cohesion at the inner centromere remained in hMis14 and HP1-α RNAi cells, whereas whole chromosome cohesion was abolished in hSgo1 RNAi cells. Thus, the hMis14 and HP1-α proteins seem to specifically affect sister centromeric cohesion, whereas hSgo1 affects whole sister chromatid cohesion.

hMis14 mutants are deficient in the enrichment of HP1-α and hSgo1 at the inner centromere

To determine rigorously whether the RNAi knockdown of hMis14 was the only factor causing the deficiency in HP1-α recruitment, a rescue experiment was performed using a chromosomally integrated GFP–HP1-α HeLa cell line and a plasmid that expressed mCherry-tagged hMis14, which is resistant to RNAi. The experimental scheme is depicted in Fig. 4 A. HeLa cells were first transfected with the mCherry-hMis14 WT gene plasmid and, 2 h later, the knockdown of endogenous hMis14 expression with hMis14 RNAi was initiated. 48 h later, the GFP–HP1-α and hSgo1 signals showed a normal localization in the mCherry-hMis14 WT–transfected cells (Fig. 4 B, top). In control HeLa cells that were not transfected with the mCherry-hMis14 plasmid, endogenous hMis14 was depleted (Fig. 4 B, bottom; and Fig. S2 D). Collectively, these results suggest that the depletion of hMis14 causes lack of enrichment of HP1-α (also hSgo1) in the inner centromere.

Next, we examined enrichment for HP1-α at the inner centromere in hMis14 m2E and m2A mutants using the protocol described in Fig. 4 A. To compare the degree of HP1 enrichment at the inner centromere, several metaphase spread chromosomes were observed, and the data were quantified. The mCherry-hMis14 m2E or m2A mutants were localized at the kinetochore, but both mutants failed to restore the enrichment in GFP–HP1-α and hSgo1. When hMis14 RNAi cells were transfected with hMis14 m2E or m2A plasmids, only 49% ($n = 660$) or 41% ($n = 310$) of chromosomes, respectively, showed GFP–HP1-α and hSgo1 signals. (Fig. 4 C, the fourth through the seventh columns). In contrast, the expression of mCherry-tagged hMis14 WT in hMis14 RNAi cells restored the inner centromeric GFP–HP1-α and hSgo1 signals in 95% ($n = 565$) of chromosomes (Fig. 4 C, third column), and the signal levels were comparable with those of control RNAi cells transfected with the vector plasmid mCherry (88%; $n = 351$; Fig. 4 C, first column). When hMis14 RNAi cells were transfected with vector plasmid mCherry, only 25% ($n = 359$) of chromosomes showed GFP–HP1-α and hSgo1 signals (Fig. 4 C, second column). Micrographs displaying many metaphase chromosomes are shown in Fig. S2 E. These results demonstrate that the hMis14 mutants are recruited to kinetochores and that the mutants impair the enrichment of HP1-α and hSgo1 at the inner centromere during mitosis.

The hMis14 mutant fails to enrich aurora B at the inner centromere

To explore whether the inner centromeric localization of aurora B was under the control of hMis14, we used the tetracycline-inducible Flip-In system to generate four stable cell lines that expressed Flag-mCherry (vector) or Flag-mCherry–tagged hMis14 WT, m2E mutant, or m2A mutant, all of which were siRNA resistant (Fig. 5 A). Tetracycline was added (0 h) to induce the expression of these chromosomally integrated WT and mutant hMis14 transgenes, and endogenous hMis14 was depleted by simultaneous siRNA. At 48 h, the level of endogenous hMis14 protein (Fig. 5 B, single asterisk) was greatly diminished, whereas the induced Flag-mCherry fusion proteins (Fig. 5 B, double asterisk) were intensely expressed. In the control RNAi cells expressing Flag-mCherry (vector), both aurora B and hSgo1 were enriched at the inner centromere (Fig. 5 C, first column), whereas both proteins were diffusely distributed along the chromosomes after hMis14 RNAi (Fig. 5 C, second column). As expected, the expression of Flag-mCherry–tagged hMis14 WT in hMis14 RNAi cells restored the inner centromeric aurora B and hSgo1 signals (Fig. 5 C, third column). In contrast, the hMis14 m2E and m2A mutant proteins failed to restore both aurora B and hSgo1 enrichment in most of the chromosomes (Fig. 5 C, fourth and fifth columns, respectively). Thus, the hMis14 mutants prevented the proper enrichment of aurora B as well as HP1-α and hSgo1 at the inner centromere. The hMis14 did not seem to affect the phosphorylation of H3 Ser10 because the immunostain signal for phosphorylated H3 Ser10 was abundant in both WT and mutant forms (Fig. S2 F).

The localization of various kinetochore proteins is hMis14 dependent

Next, various kinetochore proteins were examined to assess whether their localization was altered in hMis14 RNAi cells.

anti-hMis14 antibody after hMis14 or control RNAi (bottom). (B) Interphase HeLa cells stably expressing GFP–HP1-α were stained with anti–CENP-B antibodies after hMis14 RNAi or control RNAi. Higher magnification views of the boxed areas are shown to the right. (C) HeLa cells stably expressing GFP–HP1-α were cultured for 46 h after hMis14 RNAi or control RNAi and for an additional 2 h after the addition of nocodazole and MG132. Spread chromosomes were stained with anti-hSgo1 and anti–CENP-B antibodies. Cross section images were deconvolved and stacked. Nondeconvolved images are shown for hSgo1. (D) Spread chromosomes were stained with anti-hSgo1 antibodies after hMis14, HP1-α, and hSgo1 RNAi. Representative spreads are shown ($n = 100$). Insets show a higher magnification view of a representative chromosome. Bars, 10 μm.

Published March 15, 2010

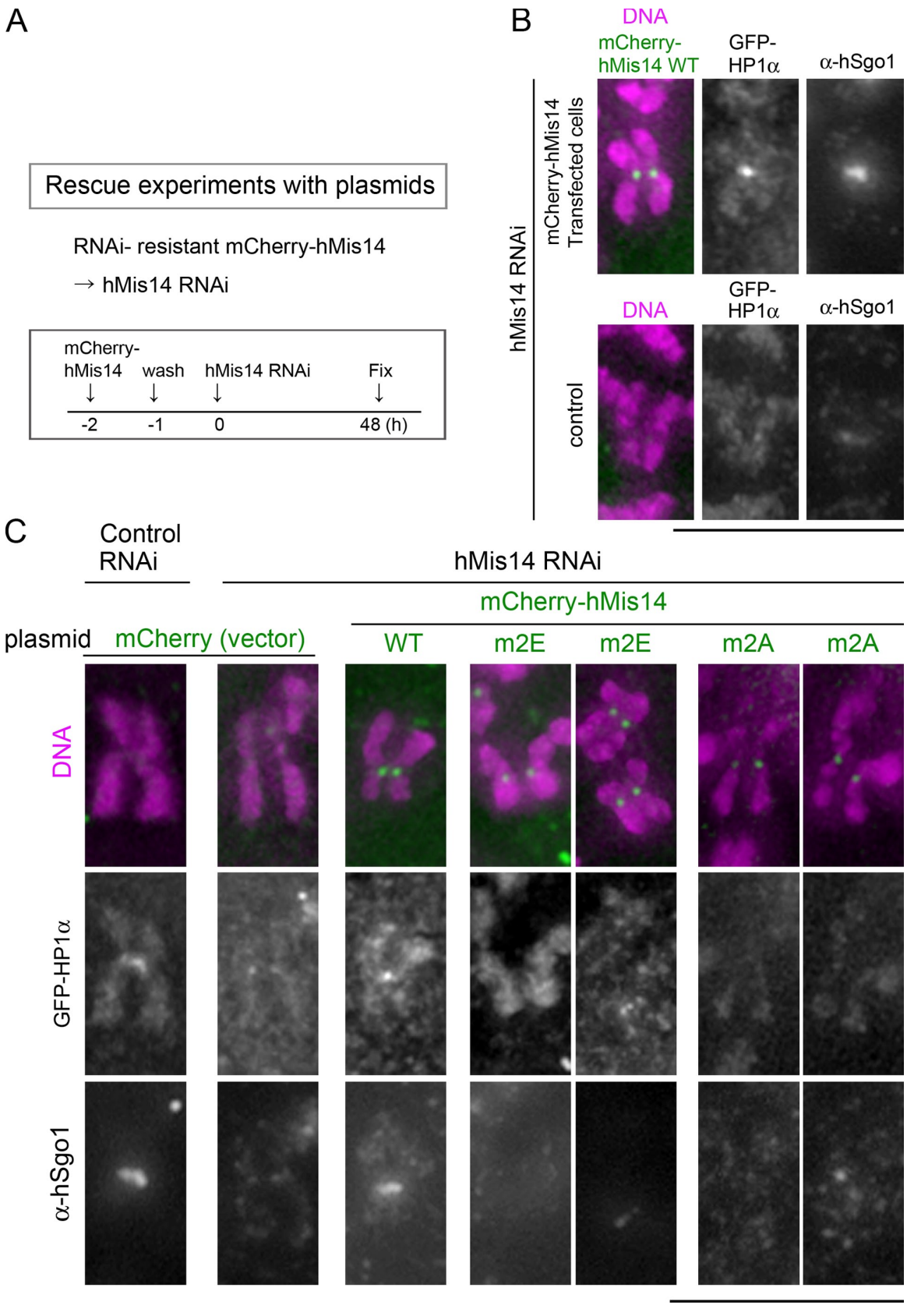

Figure 4. **hMis14 m2 mutants fail to restore GFP–HP1-α at the inner centromere.** (A) Schematized experimental procedure of the rescue experiment. See "hMis14 mutants are deficient in the enrichment of HP1-α and hSgo1 at the inner centromere" for details. (B) Spread chromosomes were stained with anti-hSgo1 antibodies. Control HeLa cells that were not transfected with mCherry-hMis14 (bottom) and mCherry-hMis14–transfected cells (top) were observed in the same field. (C) GFP–HP1-α–expressing HeLa cells were treated according to the procedures depicted in A, using plasmids as indicated. Nocodazole and MG132 were added for the last 2 h. Spread chromosomes were stained with anti-hSgo1 antibodies and Hoechst 33342 (magenta). Bars, 10 µm.

Published March 15, 2010

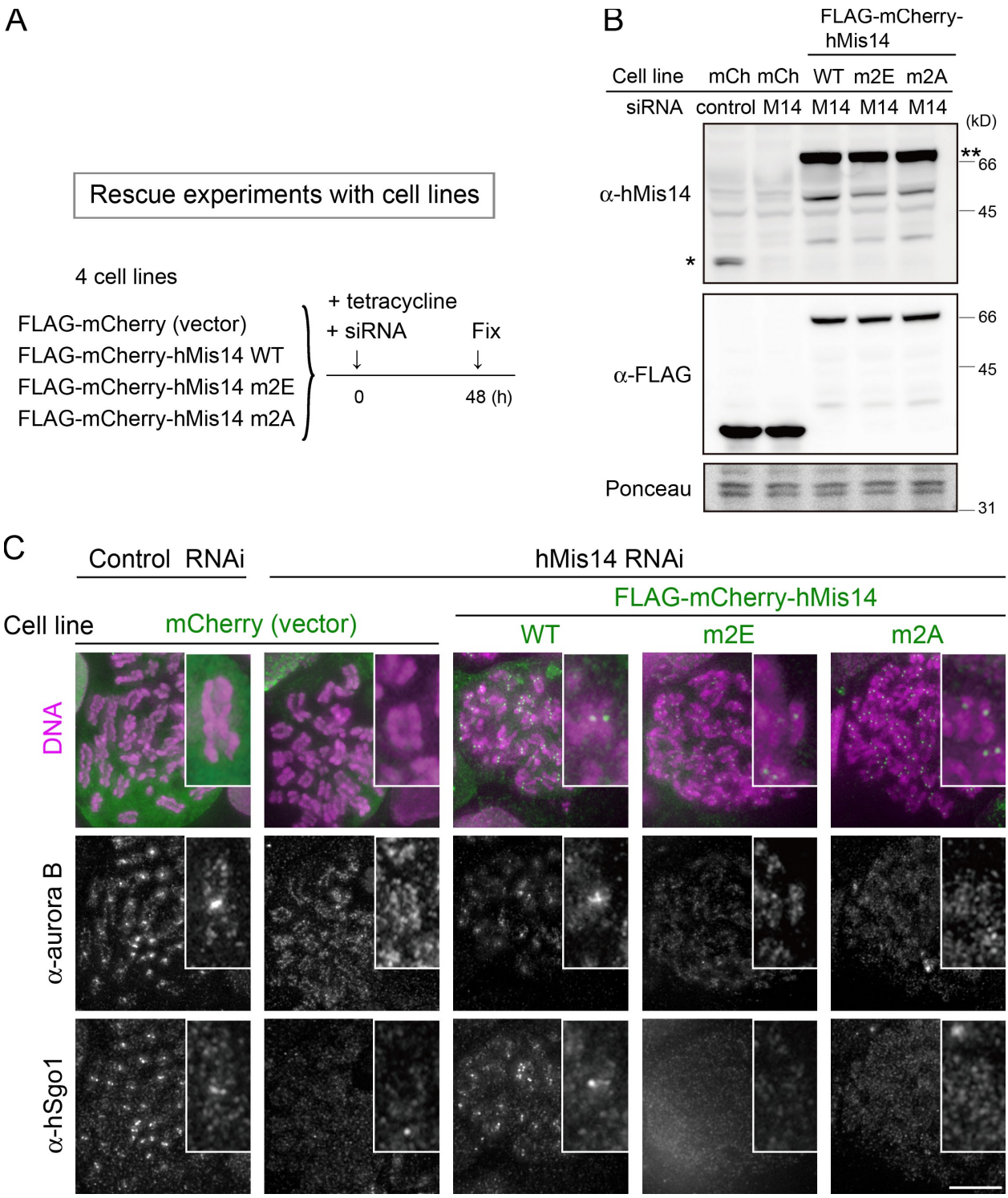

Figure 5. **hMis14 m2 mutants fail to restore aurora B at the inner centromere.** (A) Schematized experimental procedure of the rescue experiment. Four stable cell lines were generated using the Flip-In system. (B) Immunoblot of hMis14, Flag, and Ponceau staining after treatment with tetracycline and siRNA as indicated. The bands indicated by one or two asterisks represent endogenous hMis14 or exogenous Flag-mCherry (mCh)–tagged hMis14, respectively. (C) The substitute experiment was performed according to the procedures depicted in A using the cell lines indicated. Spread chromosomes were stained with the antibodies indicated. Insets show a higher magnification view of the chromosomes. Bar, 10 μm.

Although CENP-A and -C remained at the kinetochore, other kinetochore signals such as those for hMis12, hMis13, blinkin, and checkpoint proteins Bub1, BubR1, and Mad2 were all found to be abolished (Fig. S3, A–F). The hMis12 complex containing the hMis13 and hMis14 subunits directly interacted with blinkin, which binds to Bub1 and BubR1. The CENP-A and -C recruitment mechanisms seemed to be independent of hMis14.

Published March 15, 2010

Diminished kinetochore localization of hMis14 m2 mutant protein

To examine whether the hMis14 mutant protein was recruited to kinetochores and interphase centromeres, we determined the localization of hMis14 WT and m2E mutant proteins as described in Fig. 5 A. In this rescue experiment, the expression levels of the hMis14 WT and m2E proteins were comparable (Fig. 5 B). Both WT and mutant m2E mCherry-hMis14 signals were observed at the kinetochores, but the intensity of the mutant m2E signal was considerably lower than that of the WT (Fig. 6 A), showing a level of m2E signal at the kinetochores of ∼40% of that of WT in spread chromosomes (Fig. 6 B and Fig. S3 G). The same results were obtained when the intracellular GFP-hMis14 WT and m2E signals were compared in living cells (Fig. S4, A–C). The protocol used in Figs. 4 A and 5 A was used to examine whether the hMis14 m2E properly recruited hMis13, blinkin, Bub1, and BubR1 to kinetochores. The hMis14 m2E protein was able to restore kinetochore localization of all of these proteins (Fig. 6 A and Fig. S3 H). These results were consistent with the Y2H data of hMis13 and blinkin in the hMis14 m2E mutant.

To gain information about the state of endogenous hMis12 complex in the hMis14 WT and m2E mutant cell extracts, chromatin fractionation was performed. Nocodazole-arrested cell extracts treated with buffer containing 100 mM NaCl were centrifuged. Immunoblotting was performed to assay the protein levels in the pellet and supernatant fractions. In the hMis14 m2E extracts, the majority of hMis12, hMis13, and blinkin was solubilized, whereas ∼50% of them remained in the pellet fraction in the hMis14 WT extracts (Fig. 6 C). In contrast, a large amount of CENP-C remained in the pellet fraction in both extracts. In the hMis14 m2E mutant cells, the assembly of the hMis12 complex and blinkin into kinetochores appeared to be significantly impaired.

Centromeric localization of hMis14 m2 in interphase is diminished

To investigate the recruitment of the hMis14 mutant protein to interphase centromeres, HeLa cell lines stably expressing GFP-hMis14 WT or mutant m2E were constructed by chromosomal integration. The levels of ectopically expressed GFP-hMis14 bands were roughly similar to that of endogenous hMis14 (Fig. S4 A). The centromeric dot signals of GFP-hMis14 m2E during interphase were weaker (∼30%; $n = 20$; Fig. S4 D) than those of WT GFP-hMis14 (Fig. 6 D). Quantified supporting data in Fig. S4 B show two HeLa lines differently color labeled by transfecting plasmids that carried mCherry or CFP, which were mixed and observed in the same microscope field.

We then performed the chromatin fractionation of extracts from an AS culture that was mostly in interphase. After the first fractionation, the pellet fraction was treated with a buffer containing 100–500 mM NaCl, and the protein levels in the pellet and supernatant fractions were assayed (Fig. 6 E). Approximately 50% of GFP-hMis14 WT remained in the pellet after 500 mM NaCl treatment, whereas GFP-hMis14 m2E but not HP1-α was completely solubilized in all NaCl concentrations examined, showing that hMis14 m2E was more soluble than WT during interphase as well as mitosis.

The hMis14 m2E mutant causes misalignment and abnormal anaphase

To examine whether mitotic progression becomes abnormal when the interaction between hMis14 and HP1 is impaired, the substitution experiment depicted in Fig. 7 A was performed. At 48 h, the level of endogenous hMis14 protein was greatly diminished, whereas the introduced GFP fusion proteins were clearly expressed (Fig. 7 B).

To measure the timing of anaphase and monitor the alignment at metaphase, several videos were taken to visualize chromosomes using Hoechst 33342 in live cells. As shown in Fig. 7 C, control cells transfected with the GFP vector showed few defects (0% accelerated mitosis, 10% misaligned, and 0% abnormal anaphase; Fig. 7 D). However, the hMis14 RNAi cells transfected with the vector GFP plasmid showed abnormal mitosis (25% accelerated mitosis and 100% misaligned and lagging chromosomes). Therefore the alignment, anaphase onset, and progression were aberrant in hMis14 RNAi–treated cells. These RNAi phenotypes were largely rescued by plasmids carrying the GFP-hMis14 WT. In contrast, misaligned chromosomes and abnormal anaphase were still frequent (83% and 67%, respectively) when the GFP-hMis14 m2E mutant plasmid was used (Fig. 7 C and Fig. S4 E). However, the frequency of accelerated mitosis was reduced to a negligible level (4%). Misalignment and missegregation were still present in the hMis14 m2E mutant as a result of the defect in the interaction between HP1 and hMis14. These results are consistent with the fact that Bub1 and BubR1 are present at the kinetochore in hMis14 m2E cells.

HP1 RNAi causes a decrease in hMis14 in the kinetochore and the absence of hSgo1 in the inner centromere

To examine whether HP1 depletion leads to aberrant inner centromere formation and/or chromosome missegregation, HP1 RNAi was performed. Although the protein levels of HP1-α were greatly diminished, the levels of HP1-γ partly remained 72 h after the double RNAi of HP1-α and -γ (Fig. 8 A). Several videos were taken to monitor the alignment of metaphase chromosomes. In control RNAi cells, the chromosomes properly aligned and entered anaphase ∼30 min after nuclear envelope breakdown (mean duration 27 min; $n = 30$; Fig. 8 B). In contrast, in HP1-α+γ RNAi cells, the chromosomes did not align promptly (Fig. 8 C, second column), and 48% and 13% ($n = 23$) of cells showed misaligned and lagging chromosomes as indicated by arrows and arrowheads, respectively. 26% of HP1-α+γ RNAi cells showed severe misalignments and prolonged delay (Fig. 8 C, bottom), suggesting that HP1 is required for proper chromosome alignment and mitotic progression.

To examine the inner centromere structure after HP1 RNAi, mitotic spread chromosomes were observed. A significant population of cells (40%; $n = 50$) contained paired sister chromatids without primary constriction after HP1-α+γ RNAi. We speculated that these chromosomes were associated with arm cohesion, whereas sister inner centromeres were largely disconnected. For single HP1-α RNAi, a similar frequency of

Published March 15, 2010

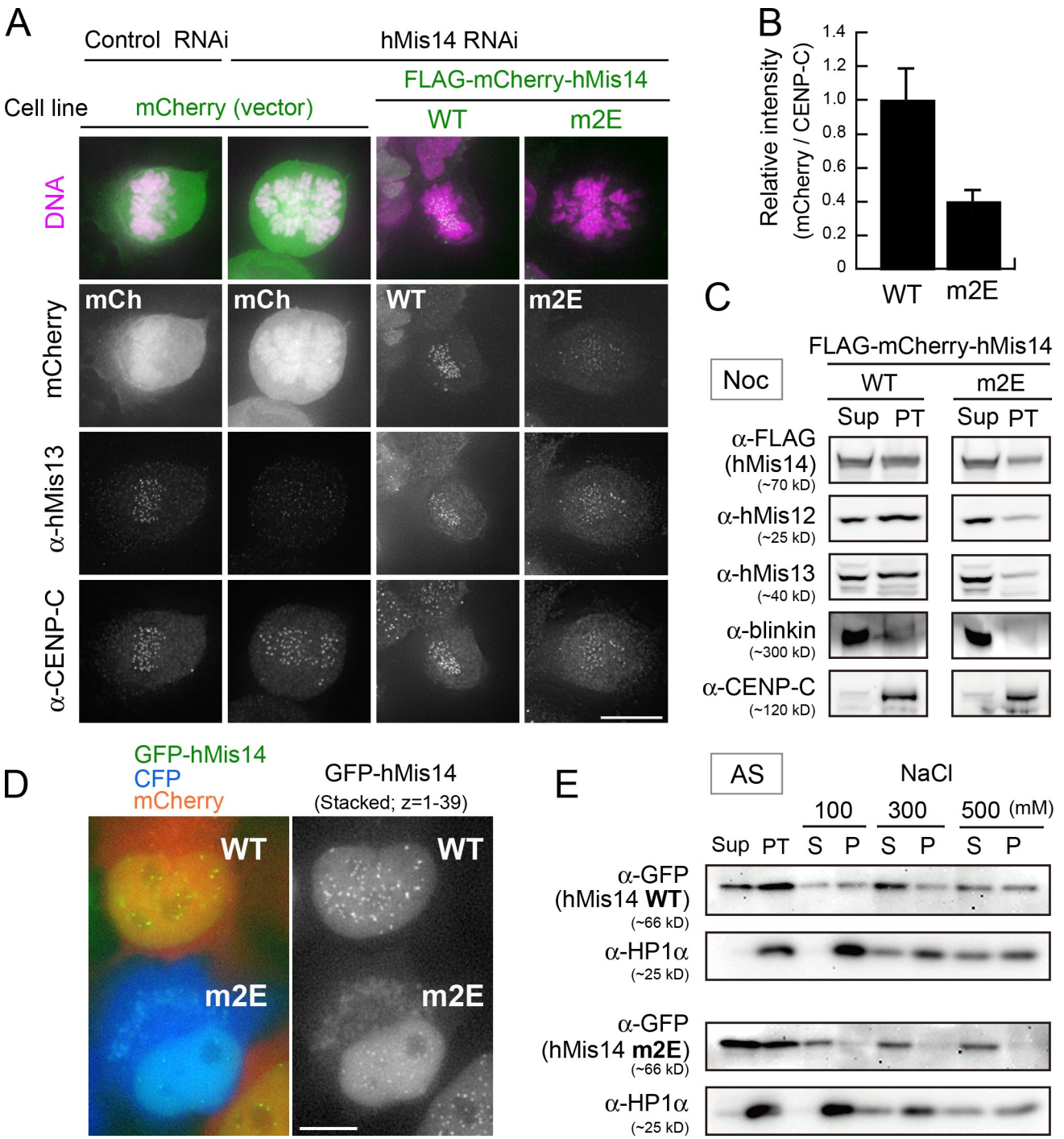

Figure 6. **Failure of the hMis14 m2E mutant to localize at the mitotic kinetochore and interphase centromere.** (A) The substitute experiment was performed according to the procedures depicted in Fig. 5 A using the cell lines indicated. Cells were fixed and stained with the antibodies indicated. mCh, mCherry. (B) Intensity of the kinetochore signals of Flag-mCherry hMis14 WT or m2E relative to that of CENP-C. 30 kinetochore signals from three cells were measured for each sample. Error bars represent standard deviation. (C) Chromatin fractionation assay. Nocodazole (Noc)-arrested extracts of cells that expressed Flag-mCherry hMis14 WT or m2E were fractionated. The supernatant (Sup) and pellet (PT) fractions were immunoblotted using the antibodies indicated. (D) Simultaneous imaging of GFP-hMis14 WT and m2E mutant in double thymidine–arrested cells. See "Centromeric localization of hMis14 m2 in interphase is diminished" for details. Cross section images were deconvolved and stacked (right). (E) Chromatin fractionation assay. AS HeLa cell extracts stably expressing GFP-hMis14 WT or m2E were used. Sup and PT stand for the supernatant and pellet fraction, respectively, of the first fractionation. S and P stand for supernatant and pellet fraction, respectively, of the second fractionation. See "Centromeric localization of hMis14 m2 in interphase is diminished" for details. Bars, 10 μm.

cells (48%; $n = 50$) revealed such aberrant chromosomes but rarely in control RNAi (4%; $n = 50$). Note that CENP-B signals (green) remained intense in these partially separated, paired sister chromatids (Fig. 8 D, middle and bottom). CENP-C (an inner kinetochore protein) signals were also intense (Fig. 8 F, bottom). Thus, the sister inner centromeres that were formed

Published March 15, 2010

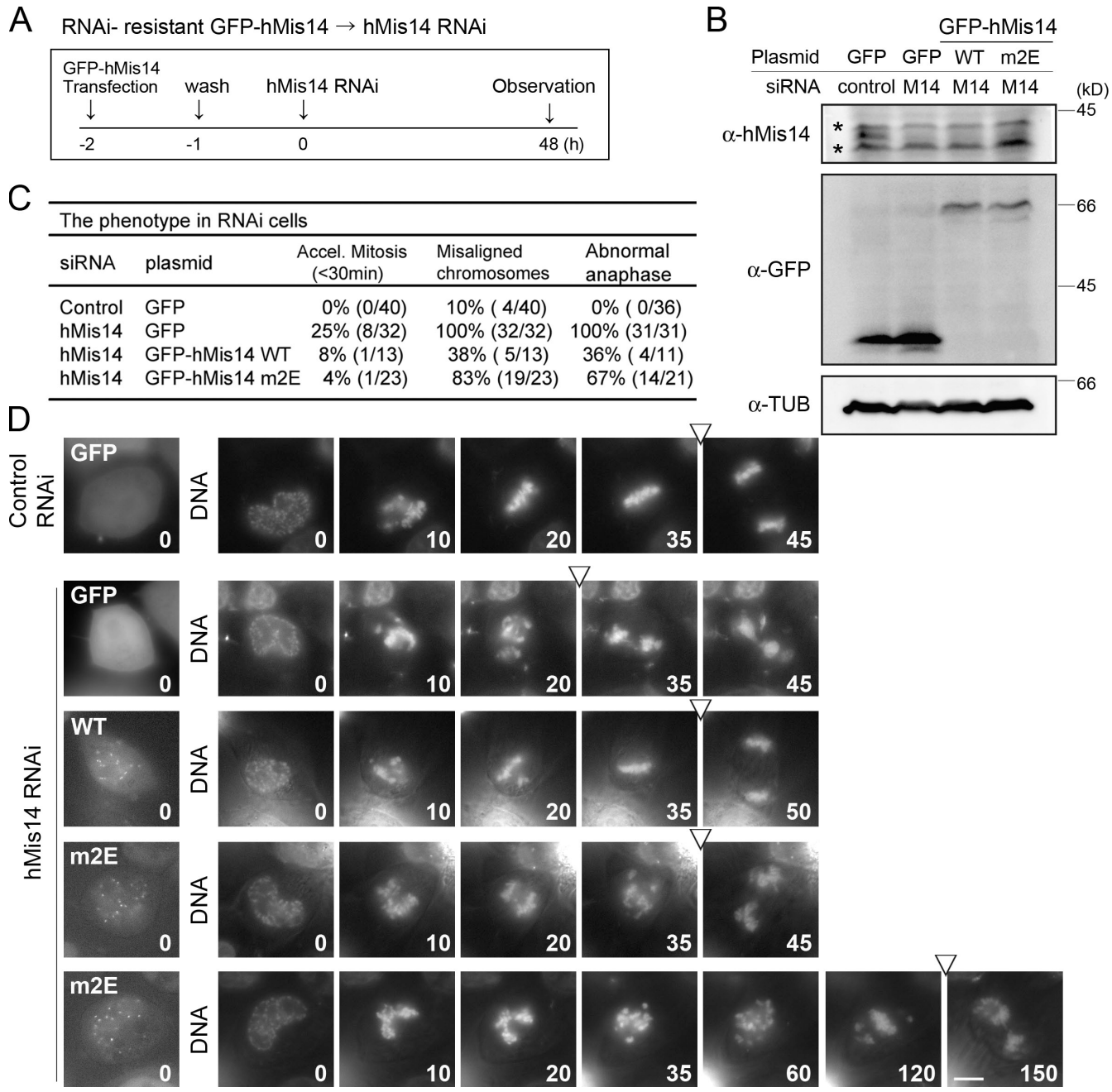

Figure 7. **The hMis14 m2E mutant fails to suppress chromosome misalignment.** (A) Schematized experimental procedures. See "The hMis14 m2E mutant causes misalignment and abnormal anaphase." (B) Immunoblot of hMis14, GFP, and tubulin (TUB) in transfected HeLa cells. The bands indicated by an asterisk are contaminating proteins that cross react with anti-hMis14 antibodies. (C) Summary of phenotypes in four different RNAi cells. (D) Time-lapse micrographs of HeLa cells. GFP and GFP-tagged RNAi-resistant hMis14 WT or m2E mutant were expressed in hMis14 RNAi cells. The numbers and arrowheads indicate the time (minutes) and the timing of anaphase onset, respectively. Bar, 10 μm.

might be partial and defective in their full association. Consistent with this notion, the signals for aurora B and hSgo1 were not enriched at all in the inner centromeres and were instead broadly diffused along the chromosomes in the single HP1-α RNAi cells (Fig. 8 E, second column). Collectively, these results suggest that the normal connection between sister inner centromeres is disrupted under HP1-α RNAi, whereas arm cohesion might partly or fully remain. Of note, the RNAi cells of aurora B displayed partially separated sister chromatids similar to those of HP1 RNAi cells (Kawashima et al., 2007).

We then examined the kinetochore levels of hMis14 under RNAi of HP1-α+γ or HP1-α. The relative intensities of the hMis14 to CENP-C signals were significantly reduced (25%; $n = 40$; and 36%; $n = 40$) after HP1-α+γ and HP1-α RNAi, respectively (Fig. 8, F and G). In interphase, the centromere localization of GFP-hMis14/DC8 is also diminished after the double RNAi of HP1-α and -γ (Supplementary Information, Fig. S5 in Obuse et al., 2004). These results are consistent with the mutual dependence of HP1 and hMis14 for their localization and function.

Published March 15, 2010

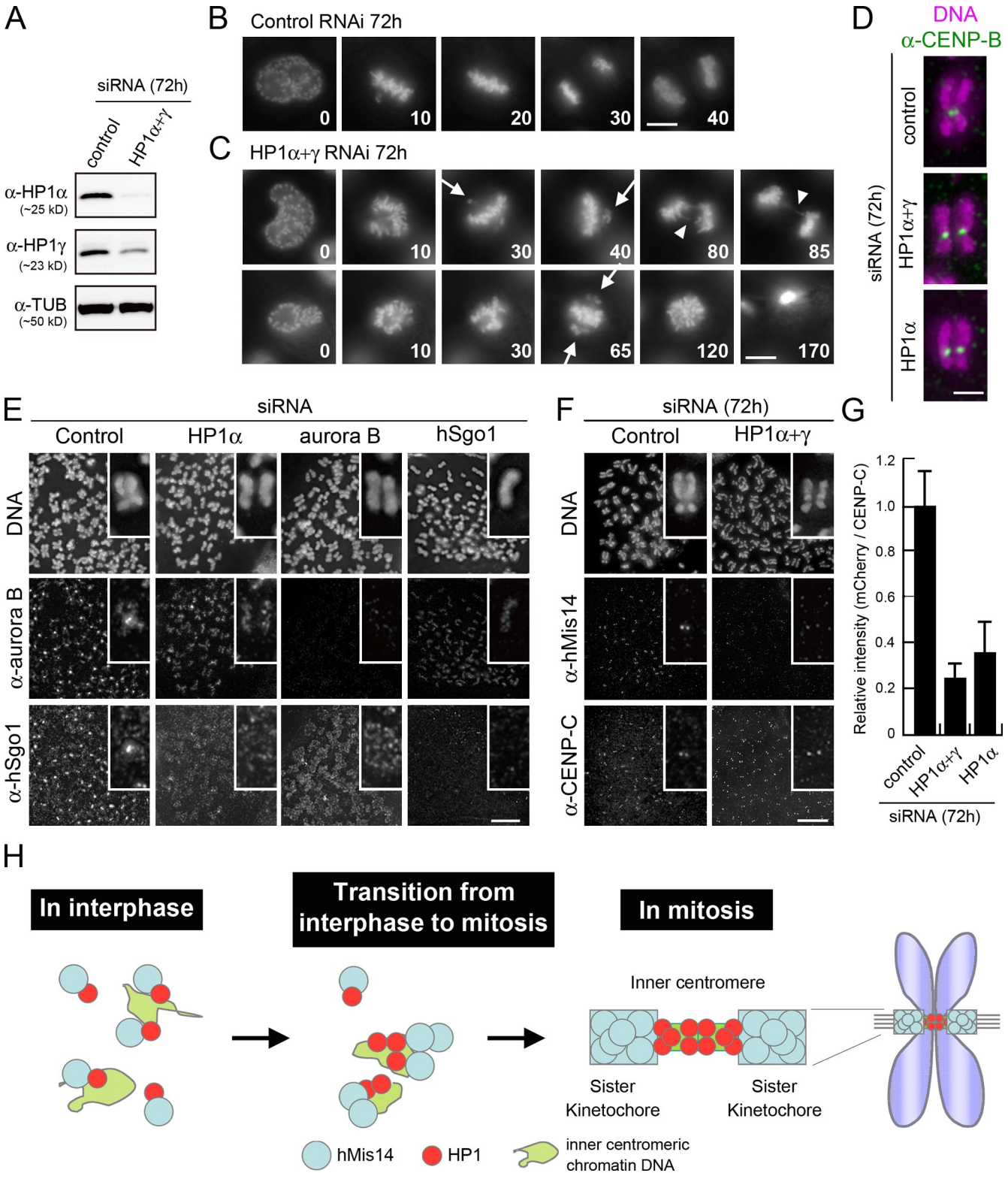

Figure 8. **HP1 RNAi prevents the proper formation of the inner centromere and the kinetochore localization of hMis14.** (A) Immunoblot of HP1-α and -γ after RNAi. The loading control was tubulin (TUB). (B and C) Time-lapse micrographs of HeLa cells stably expressing histone H2B–GFP after control RNAi (B) and HP1-α+γ RNAi (C). The number indicates the time (minutes). Arrows and arrowheads indicate misaligned and lagging chromosomes, respectively. (D) Mitotic spread chromosomes were stained with anti–CENP-B antibodies and Hoechst 33342 (magenta) after HP1-α+γ and HP1-α RNAi. (E) Spread chromosomes were immunostained with anti–aurora B and anti-hSgo1 antibodies after HP1-α, aurora B, and hSgo1 RNAi. (F) Spread chromosomes were immunostained with anti-hMis14 and anti–CENP-C antibodies after HP1-α+γ RNAi. (E and F) Insets show a higher magnification view of a representative chromosome. (G) The intensity of kinetochore signals of hMis14 relative to that of CENP-C was measured after HP1 RNAi. 40 kinetochore signals from four cells were measured for each sample. Error bars represent standard deviation. (H) A model of the inner centromere formation by hMis14 and HP1. See Discussion. Bars: (B, C, E, and F) 10 μm; (D) 2 μm.

Published March 15, 2010

Discussion

In this study, we show that the human kinetochore protein hMis14, a component of the heterotetrameric hMis12 complex, directly binds to the CSD of heterochromatin protein HP1. Although this binding occurs during interphase, it is required for the mitotic formation of the inner centromere, the region where sister kinetochores are connected and cohesins are abundant but where hMis14 is absent. This dependence of the cell cycle regulation on the HP1–hMis14 interaction is discussed in this section. HP1 is known to play a role in heterochromatin formation (Eissenberg and Elgin, 2000) and function as an adaptor by bringing together different chromatin proteins into complexes via protein–protein interactions with the CD and the CSD domains (Quivy et al., 2004; Thiru et al., 2004). HP1 is highly enriched in the inner centromere of mitotic chromosomes, but the reason for this enrichment is not well understood. The Mis14 protein family in the mitotic kinetochore is evolutionarily conserved (Meraldi et al., 2006; Przewloka et al., 2007). *Saccharomyces cerevisiae* Nsl1, *Schizosaccharomyces pombe* Mis14, and hMis14/hNsl1/DC8 all belong to the Mis14 family of proteins, although their sequence identity is low (~20–25%). The conserved sequences observed across species, including vertebrates, flies, and worms, reside in the central region of the proteins.

We show that the hMis14 protein is a tripartite-binding protein that directly interacts with HP1 and two other kinetochore proteins, hMis13 (another subunit of the hMis12 complex) and blinkin (an Spc105-like kinetochore protein bound to the spindle assembly checkpoint proteins Bub1 and BubR1). The HP1-binding region of hMis14 is sandwiched by two other binding sequences (Fig. 1 G). Note that the HP1-binding consensus PXVXL is found only in vertebrates (see last paragraph of Discussion). The interaction between HP1 and hMis14 is characterized by two features. First, the interaction occurs during interphase but apparently not during mitosis. Second, the interaction requires only small domains: the CSD-containing fragment of HP1 directly interacts with the 25-aa fragment of hMis14, which contains a CSD-binding PXVXL motif.

The functional analyses performed in this study revealed that the formation of the inner centromere of human mitotic chromosomes requires hMis14, implying that the interphase interaction between HP1 and hMis14 becomes crucial in mitosis. The inner centromeric localization of HP1-α, hSgo1, and aurora B was diminished, and the resulting inner centromere was only partially assembled when WT hMis14 was substituted by a mutant m2 protein that specifically lacked the ability to interact with HP1. The partial sister inner centromeres containing CENP-B were observed as double dots and failed to form the primary constriction. As the hMis14 m2 mutant protein normally binds to blinkin and hMis13, localization defects of HP1-α in the hMis14 m2 mutant strain would be solely caused by the absence of a PXVXL motif–mediated interaction between HP1-α and hMis14.

During interphase, hMis14 bound to the centromere may recruit a subpopulation of HP1 as interacting partner. The hMis14–HP1 complex in interphase centromeric chromatin is possibly the basis for initiating the formation of the inner centromere upon mitosis. However, structural changes must take place so as to dissociate hMis14 from HP1 during the assembly of the separate structures, namely the inner centromere and kinetochore, with the boundary interface between them. This "dynamic remodeling" hypothesis in the transition between interphase and mitosis is depicted in Fig. 8 H. Because hMis14 is the stable subunit of the Mis12 heterotetrameric complex, we presume that hMis14 acts as the subunit of the complex during the hypothetical assembly.

The results of the functional analyses also revealed that HP1-α inversely affects the localization and function of hMis14 at the mitotic kinetochore. The interdependence of these proteins for their recruitment to the mitotic kinetochore and inner centromere explains several findings in this study. The hMis14 m2E mutant protein and also endogenous hMis14 in HP1 RNAi cells were significantly diminished at the kinetochore. In addition, a large proportion of hMis13 and blinkin became solubilized in the hMis14 mutant–expressing cells, probably causing the assembly of an unstable Mis12–blinkin complex and leading to the chromosome misalignment observed. Thus, the inner centromere affects kinetochore functions. We showed in this study that the interphase interaction between hMis14 and HP1-α is essential for the proper assembly of HP1 in the inner centromere and also of hMis14 in the kinetochore in subsequent mitosis, but its mechanism, perhaps regulated in the cell cycle, remains to be determined.

The hMis14 mutant specifically prevented the enrichment of HP1-α at the inner centromere but not in the arm regions, as shown by the GFP–HP1-α dim signals along the chromosome and lack of accumulation at the inner centromere. Consistently, hMis14 mutants did not cause the complete sister chromatid separation observed in hSgo1 RNAi cells. Our results suggest that hMis14 may specifically recruit HP1 to the inner centromere through the PXVXL-mediated interaction.

Because hMis14 is absent from the inner centromere of mitotic chromosomes, the enrichment mechanism of HP1 at the inner centromere must involve its dissociation from hMis14 (Fig. 8 H). A mechanism similar to that taking place in heterochromatic spreads (Talbert and Henikoff, 2006; Grewal and Jia, 2007) may be responsible for the separation of HP1 from hMis14, the HP1 deposition along inner centromeric DNA, and the formation of the boundary between the kinetochore and the inner centromere. The HP1–hMis14 complex possibly acts as the seed to initiate the dissemination in the opposite directions for inner centromere and kinetochore. Because the inner centromere and kinetochore DNAs may consist of the same α-satellite DNA sequences in human chromosomes, the model described here is conceivable as the spreading might occur on the same type of satellite DNA sequences. Although we favor the aforementioned model, there are other existing models to explain this phenomenon that suggest that the interphase association of hMis14 with HP1 might not be mechanistically linked to its role in the mitotic kinetochore formation. These models suggest that their relations might be independent because of a yet uncovered cell cycle–regulated function of hMis14. Although further study is required for a better understanding of this issue, hMis14 is

Published March 15, 2010

nevertheless revealed as a key controlling element for the formation of the inner centromere and kinetochore in the human chromosome. The trident-binding nature of hMis14 explains the behavior of various kinetochore proteins in the hMis14 mutants used in this study.

The PXVXL motif and surrounding amino acids are well conserved in mammalian and chicken Mis14 proteins but are not found in other vertebrates such as fish (Fig. S5 A). The motif has also not been found in fly, worm, or fungi, showing that the PXVXL motif is not well conserved across different organisms. For example, TIF1-α, a well-studied HP1-binding protein, is evolutionarily conserved, whereas the PXVXL motif is only found in organisms higher than birds (Fig. S5 B), suggesting that a motif other than PXVXL might exist for HP1 binding in other organisms. A clarification of this issue in terms of the evolution of the inner centromere requires further bioinformatic investigations. In *S. pombe*, the HP1-like proteins Swi6 and Chp2 that contain the CD and CSD domains (Ekwall et al., 1995; Sadaie et al., 2008) bind to the repetitive heterochromatic pericentromeric DNAs that might form an inner centromere-like structure during mitosis (Takahashi et al., 1992), and spMis14 binds to different central centromeric DNAs that associate with kinetochore proteins, including Mis12 and CENP-A–like Cnp1 during mitosis. However, the interaction between Swi6 and spMis14 has not been detected during interphase. It remains to be determined whether fungal chromosomes contain an inner centromere similar to that in higher eukaryotes.

Materials and methods

Strains and media

HeLa cells and strains that stably express GFP-hMis14 WT, GFP-hMis14 m2E mutant, GFP–HP1-α, or histone H2B–GFP were grown at 37°C in DME (Kohjin Bio) supplemented with 10% FBS (Biowest), 1% penicillin-streptomycin, and 1% antibiotic and antimycotic (Invitrogen; Goshima et al., 2003). Cells were treated with 100 ng/ml nocodazole (MP Biomedicals) and 20 µM MG132 (EMD). HeLa cell lines that stably expressed GFP-hMis14 WT, GFP-hMis14 m2E mutant, or GFP–HP1-α (gift from R. Nozawa, Hokkaido University, Kita-ku, Sapporo, Japan) were isolated as previously described (Obuse et al., 2004). Stable Flip-In TRex 293 cells (Invitrogen) were constructed according to the manufacturer's protocol. To induce transgenes, cells were incubated with 1 µg/ml tetracycline (MP Biomedicals).

Plasmids and transfection

The cDNA genes for hMis14 and HP1 were previously isolated (Obuse et al., 2004). The mutated hMis14 cDNAs were made by site-directed mutagenesis. To construct RNAi-resistant hMis14, the nucleotide sequence 5′-CGGGCTGTGACCGAAATGCTACAA-3′ was changed to 5′-CGCGCAGTCACAGACATGCTGCAG-3′. All of the mutations were verified by DNA sequencing. Plasmid DNAs purified using an Endofree Maxi kit (QIAGEN) were transfected into HeLa cells using the Effectene transfection kit (QIAGEN).

The RNAi method

siRNAs were transfected with Lipofectamine RNAi MAX (Invitrogen). The cell culture and transfection of siRNA were performed according to the manufacturer's instructions. The stealth siRNA oligonucleotide HSS119542 for hMis14/C1orf48 was purchased from Invitrogen. HP1-α, HP1-γ (Obuse et al., 2004), aurora B (Ditchfield et al., 2003), and hSgo1 (Kitajima et al., 2005) were purchased from J-BioS. Scrambled stealth siRNA and luciferase siRNA were used as controls. RNAi cells were fixed and observed at the indicated times after transfection.

Y2H analysis

The two-hybrid analysis was performed according to the procedures described in the two-hybrid analysis kit (MATCHMAKER; Takara Bio Inc.) using plasmids pGBT9 and pGAD424. The β-galactosidase filter assay was performed using the SFY526 strain that carried the GAL1-lacZ reporter as described in the manufacturer's instructions (Takara Bio Inc.).

Antibodies

Monoclonal antibodies against hMis14 (hMis14/DC8 S#2) and hMis13 (S#18) were raised using the N-terminal 19 aa and C-terminal 19 aa as the antigens, respectively. Immunoblots and immunofluorescence experiments were performed using the following antibodies: hMis12 (anti–rabbit 1:30), CENP-A (A3 anti–mouse 1:100), CENP-B (anti–mouse 1:2), CENP-C (anti–guinea pig 1:1,000; Goshima et al., 2003), blinkin (anti–mouse 1:20), hMis13 (anti–mouse S#18 1:20; or anti–rabbit 1:1,000; Obuse et al., 2004), Bub1 (anti–sheep 1:1,000), BubR1 (anti–sheep 1:1,000; Taylor et al., 2001), HP1-α (anti–mouse 1:500; Millipore), HP1-γ (anti–rabbit 1:500; Abcam), hSgo1 (anti–rabbit 1:1,000; gift from Y. Watanabe, University of Tokyo, Yayoi, Tokyo, Japan; Kitajima et al., 2005), AIM-1/aurora B (anti–mouse 1:500; BD), anti–histone H3S10ph (anti–rabbit 1:1,000; Abcam), Flag (anti–mouse 1:1,000; M2E; Sigma-Aldrich), GFP (anti–mouse 1:500; Roche), and tubulin (anti–mouse 1:500; DM1A; Sigma-Aldrich).

Live cell imaging and immunofluorescence

Live cell analysis was performed as previously described (Haraguchi et al., 1997). HeLa cells that stably expressed histone H2B–GFP were used for the visualization of chromatin. Cells that entered mitosis 66–72 h after HP1-α+γ siRNA transfection were observed. Transfected cells grown on glass-based dishes (IWAKI) were supplemented with 20 mM Hepes, pH 7.4, and observed using the Delta Vision RT system (Applied Precision) at a temperature of 37°C. The GFP images were taken at 1-min intervals with an exposure time of 0.2 s. Cells that entered mitosis 42–48 h after siRNA transfection were observed. For DNA staining, HeLa cells were cultured in the presence of 50 ng/ml Hoechst 33342, and the live images were taken at 5-min intervals with a LiveUV filter (Chroma Technology Corp.). Immunofluorescence microscopy was performed as previously described with the antibodies indicated (Toyoda and Yanagida, 2006; Kiyomitsu et al., 2007). DNA was counterstained by Hoechst 33342. In fixed cells, a z series of 20–40 images at 0.2-µm intervals was captured and processed using constrained iterative deconvolution. Deconvolved image stacks were projected, and fluorescence signal intensities were quantified using SoftWoRx (Applied Precision). To quantify the kinetochore fluorescent signals, we measured the intensity of >20 kinetochores and subtracted the background intensity of the region, which was measured adjacent to the kinetochores.

Mitotic chromosome spread

For the detection of GFP–HP1-α, chromosome spread analysis was performed with modifications of the method previously described (Toyoda and Yanagida, 2006). After nocodazole treatment for 3 h, cells were collected by mitotic shake off, swollen in a hypotonic solution (16.6% FBS solution), and then spread with Cytospin 4 (Thermo Fisher Scientific) at 1,300 rpm for 10 min. The area around the spread was marked with PAP-PEN (Invitrogen). Spread cells were fixed with 2% paraformaldehyde in PBS at room temperature for 15 min and permeabilized in 0.5% Triton X-100 in PBS for 5 min at room temperature. After blocking with 1% BSA in PBS, cells were incubated with primary antibodies for at least 1 h. After gentle washing, cells were incubated with secondary antibodies for at least 40 min.

Online supplemental material

Fig. S1 shows the interaction between hMis14 and HP1-α. Fig. S2 shows the restoration of inner centromere enrichment of GFP–HP1-α by hMis14 WT plasmids. Fig. S3 shows hMis14-dependent localization of hMis12, blinkin, and checkpoint proteins at kinetochores. Fig. S4 shows the simultaneous image of HeLa cells that stably express GFP-tagged hMis14 WT or the m2E mutant. Fig. S5 shows the amino acid sequence alignment of the Mis14 family of proteins. Online supplemental material is available at http://www.jcb.org/cgi/content/full/jcb.200908096/DC1.

We are greatly indebted to R. Nozawa for the GFP–HP1-α stably expressing HeLa cells, N. Nozaki for the generation of the anti-hMis14 and anti-hMis13 antibodies, and Y. Watanabe for the anti-hSgo1 antibody.

This study was supported by grants for Specially Promoted Research from the Ministry of Education, Culture, Sports, Science and Technology and the Core Research for Evolutional Science and Technology Research Program of the Japan Science and Technology Corporation and Grant-in-Aid for Young Scientists (Start-up).

Submitted: 18 August 2009
Accepted: 18 February 2010

References

Amor, D.J., P. Kalitsis, H. Sumer, and K.H. Choo. 2004. Building the centromere: from foundation proteins to 3D organization. *Trends Cell Biol.* 14:359–368. doi:10.1016/j.tcb.2004.05.009

Brasher, S.V., B.O. Smith, R.H. Fogh, D. Nietlispach, A. Thiru, P.R. Nielsen, R.W. Broadhurst, L.J. Ball, N.V. Murzina, and E.D. Laue. 2000. The structure of mouse HP1 suggests a unique mode of single peptide recognition by the shadow chromo domain dimer. *EMBO J.* 19:1587–1597. doi:10.1093/emboj/19.7.1587

Chan, G.K., S.T. Liu, and T.J. Yen. 2005. Kinetochore structure and function. *Trends Cell Biol.* 15:589–598. doi:10.1016/j.tcb.2005.09.010

Cheeseman, I.M., S. Niessen, S. Anderson, F. Hyndman, J.R. Yates III, K. Oegema, and A. Desai. 2004. A conserved protein network controls assembly of the outer kinetochore and its ability to sustain tension. *Genes Dev.* 18:2255–2268. doi:10.1101/gad.1234104

Cleveland, D.W., Y. Mao, and K.F. Sullivan. 2003. Centromeres and kinetochores: from epigenetics to mitotic checkpoint signaling. *Cell*. 112:407–421. doi:10.1016/S0092-8674(03)00115-6

Cooke, C.A., R.L. Bernat, and W.C. Earnshaw. 1990. CENP-B: a major human centromere protein located beneath the kinetochore. *J. Cell Biol.* 110:1475–1488. doi:10.1083/jcb.110.5.1475

Ditchfield, C., V.L. Johnson, A. Tighe, R. Ellston, C. Haworth, T. Johnson, A. Mortlock, N. Keen, and S.S. Taylor. 2003. Aurora B couples chromosome alignment with anaphase by targeting BubR1, Mad2, and Cenp-E to kinetochores. *J. Cell Biol.* 161:267–280. doi:10.1083/jcb.200208091

Earnshaw, W.C., and N. Rothfield. 1985. Identification of a family of human centromere proteins using autoimmune sera from patients with scleroderma. *Chromosoma*. 91:313–321. doi:10.1007/BF00328227

Eissenberg, J.C., and S.C. Elgin. 2000. The HP1 protein family: getting a grip on chromatin. *Curr. Opin. Genet. Dev.* 10:204–210. doi:10.1016/S0959-437X(00)00058-7

Ekwall, K., J.P. Javerzat, A. Lorentz, H. Schmidt, G. Cranston, and R. Allshire. 1995. The chromodomain protein Swi6: a key component at fission yeast centromeres. *Science*. 269:1429–1431. doi:10.1126/science.7660126

Fujita, Y., T. Hayashi, T. Kiyomitsu, Y. Toyoda, A. Kokubu, C. Obuse, and M. Yanagida. 2007. Priming of centromere for CENP-A recruitment by human hMis18alpha, hMis18beta, and M18BP1. *Dev. Cell*. 12:17–30. doi:10.1016/j.devcel.2006.11.002

Goshima, G., S. Saitoh, and M. Yanagida. 1999. Proper metaphase spindle length is determined by centromere proteins Mis12 and Mis6 required for faithful chromosome segregation. *Genes Dev.* 13:1664–1677. doi:10.1101/gad.13.13.1664

Goshima, G., T. Kiyomitsu, K. Yoda, and M. Yanagida. 2003. Human centromere chromatin protein hMis12, essential for equal segregation, is independent of CENP-A loading pathway. *J. Cell Biol.* 160:25–39. doi:10.1083/jcb.200210005

Grewal, S.I., and S. Jia. 2007. Heterochromatin revisited. *Nat. Rev. Genet.* 8:35–46. doi:10.1038/nrg2008

Haraguchi, T., T. Kaneda, and Y. Hiraoka. 1997. Dynamics of chromosomes and microtubules visualized by multiple-wavelength fluorescence imaging in living mammalian cells: effects of mitotic inhibitors on cell cycle progression. *Genes Cells*. 2:369–380. doi:10.1046/j.1365-2443.1997.1280326.x

Hauf, S., I.C. Waizenegger, and J.M. Peters. 2001. Cohesin cleavage by separase required for anaphase and cytokinesis in human cells. *Science*. 293:1320–1323. doi:10.1126/science.1061376

Hayakawa, T., T. Haraguchi, H. Masumoto, and Y. Hiraoka. 2003. Cell cycle behavior of human HP1 subtypes: distinct molecular domains of HP1 are required for their centromeric localization during interphase and metaphase. *J. Cell Sci.* 116:3327–3338. doi:10.1242/jcs.00635

Hayashi, T., Y. Fujita, O. Iwasaki, Y. Adachi, K. Takahashi, and M. Yanagida. 2004. Mis16 and Mis18 are required for CENP-A loading and histone deacetylation at centromeres. *Cell*. 118:715–729. doi:10.1016/j.cell.2004.09.002

Hoque, M.T., and F. Ishikawa. 2001. Human chromatid cohesin component hRad21 is phosphorylated in M phase and associated with metaphase centromeres. *J. Biol. Chem.* 276:5059–5067. doi:10.1074/jbc.M007809200

Howman, E.V., K.J. Fowler, A.J. Newson, S. Redward, A.C. MacDonald, P. Kalitsis, and K.H. Choo. 2000. Early disruption of centromeric chromatin organization in centromere protein A (Cenpa) null mice. *Proc. Natl. Acad. Sci. USA*. 97:1148–1153. doi:10.1073/pnas.97.3.1148

Kawashima, S.A., T. Tsukahara, M. Langegger, S. Hauf, T.S. Kitajima, and Y. Watanabe. 2007. Shugoshin enables tension-generating attachment of kinetochores by loading Aurora to centromeres. *Genes Dev.* 21:420–435. doi:10.1101/gad.1497307

Kitajima, T.S., S. Hauf, M. Ohsugi, T. Yamamoto, and Y. Watanabe. 2005. Human Bub1 defines the persistent cohesion site along the mitotic chromosome by affecting Shugoshin localization. *Curr. Biol.* 15:353–359. doi:10.1016/j.cub.2004.12.044

Kitajima, T.S., T. Sakuno, K. Ishiguro, S. Iemura, T. Natsume, S.A. Kawashima, and Y. Watanabe. 2006. Shugoshin collaborates with protein phosphatase 2A to protect cohesin. *Nature*. 441:46–52. doi:10.1038/nature04663

Kiyomitsu, T., C. Obuse, and M. Yanagida. 2007. Human Blinkin/AF15q14 is required for chromosome alignment and the mitotic checkpoint through direct interaction with Bub1 and BubR1. *Dev. Cell*. 13:663–676. doi:10.1016/j.devcel.2007.09.005

Kline, S.L., I.M. Cheeseman, T. Hori, T. Fukagawa, and A. Desai. 2006. The human Mis12 complex is required for kinetochore assembly and proper chromosome segregation. *J. Cell Biol.* 173:9–17. doi:10.1083/jcb.200509158

Koch, B., S. Kueng, C. Ruckenbauer, K.S. Wendt, and J.M. Peters. 2008. The Suv39h-HP1 histone methylation pathway is dispensable for enrichment and protection of cohesin at centromeres in mammalian cells. *Chromosoma*. 117:199–210. doi:10.1007/s00412-007-0139-z

Liu, S.T., J.B. Rattner, S.A. Jablonski, and T.J. Yen. 2006. Mapping the assembly pathways that specify formation of the trilaminar kinetochore plates in human cells. *J. Cell Biol.* 175:41–53. doi:10.1083/jcb.200606020

Masumoto, H., H. Masukata, Y. Muro, N. Nozaki, and T. Okazaki. 1989. A human centromere antigen (CENP-B) interacts with a short specific sequence in alphoid DNA, a human centromeric satellite. *J. Cell Biol.* 109:1963–1973. doi:10.1083/jcb.109.5.1963

Meraldi, P., A.D. McAinsh, E. Rheinbay, and P.K. Sorger. 2006. Phylogenetic and structural analysis of centromeric DNA and kinetochore proteins. *Genome Biol.* 7:R23. doi:10.1186/gb-2006-7-3-r23

Minc, E., Y. Allory, H.J. Worman, J.C. Courvalin, and B. Buendia. 1999. Localization and phosphorylation of HP1 proteins during the cell cycle in mammalian cells. *Chromosoma*. 108:220–234. doi:10.1007/s004120050372

Musacchio, A., and E.D. Salmon. 2007. The spindle-assembly checkpoint in space and time. *Nat. Rev. Mol. Cell Biol.* 8:379–393. doi:10.1038/nrm2163

Nielsen, P.R., D. Nietlispach, H.R. Mott, J. Callaghan, A. Bannister, T. Kouzarides, A.G. Murzin, N.V. Murzina, and E.D. Laue. 2002. Structure of the HP1 chromodomain bound to histone H3 methylated at lysine 9. *Nature*. 416:103–107. doi:10.1038/nature722

Obuse, C., O. Iwasaki, T. Kiyomitsu, G. Goshima, Y. Toyoda, and M. Yanagida. 2004. A conserved Mis12 centromere complex is linked to heterochromatic HP1 and outer kinetochore protein Zwint-1. *Nat. Cell Biol.* 6:1135–1141. doi:10.1038/ncb1187

Okada, T., J. Ohzeki, M. Nakano, K. Yoda, W.R. Brinkley, V. Larionov, and H. Masumoto. 2007. CENP-B controls centromere formation depending on the chromatin context. *Cell*. 131:1287–1300. doi:10.1016/j.cell.2007.10.045

Przewloka, M.R., W. Zhang, P. Costa, V. Archambault, P.P. D'Avino, K.S. Lilley, E.D. Laue, A.D. McAinsh, and D.M. Glover. 2007. Molecular analysis of core kinetochore composition and assembly in *Drosophila melanogaster*. *PLoS One*. 2:e478. doi:10.1371/journal.pone.0000478

Quivy, J.P., D. Roche, D. Kirschner, H. Tagami, Y. Nakatani, and G. Almouzni. 2004. A CAF-1 dependent pool of HP1 during heterochromatin duplication. *EMBO J.* 23:3516–3526. doi:10.1038/sj.emboj.7600362

Rieder, C.L., and E.D. Salmon. 1998. The vertebrate cell kinetochore and its roles during mitosis. *Trends Cell Biol.* 8:310–318. doi:10.1016/S0962-8924(98)01299-9

Ruchaud, S., M. Carmena, and W.C. Earnshaw. 2007. Chromosomal passengers: conducting cell division. *Nat. Rev. Mol. Cell Biol.* 8:798–812. doi:10.1038/nrm2257

Sadaie, M., R. Kawaguchi, Y. Ohtani, F. Arisaka, K. Tanaka, K. Shirahige, and J. Nakayama. 2008. Balance between distinct HP1 family proteins controls heterochromatin assembly in fission yeast. *Mol. Cell. Biol.* 28:6973–6988. doi:10.1128/MCB.00791-08

Saitoh, H., J. Tomkiel, C.A. Cooke, H. Ratrie III, M. Maurer, N.F. Rothfield, and W.C. Earnshaw. 1992. CENP-C, an autoantigen in scleroderma, is a component of the human inner kinetochore plate. *Cell*. 70:115–125. doi:10.1016/0092-8674(92)90538-N

Schueler, M.G., and B.A. Sullivan. 2006. Structural and functional dynamics of human centromeric chromatin. *Annu. Rev. Genomics Hum. Genet.* 7:301–313. doi:10.1146/annurev.genom.7.080505.115613

Smothers, J.F., and S. Henikoff. 2000. The HP1 chromo shadow domain binds a consensus peptide pentamer. *Curr. Biol.* 10:27–30. doi:10.1016/S0960-9822(99)00260-2

Sugimoto, K., H. Tasaka, and M. Dotsu. 2001. Molecular behavior in living mitotic cells of human centromere heterochromatin protein HPLalpha

ectopically expressed as a fusion to red fluorescent protein. *Cell Struct. Funct.* 26:705–718. doi:10.1247/csf.26.705

Sullivan, K.F., M. Hechenberger, and K. Masri. 1994. Human CENP-A contains a histone H3 related histone fold domain that is required for targeting to the centromere. *J. Cell Biol.* 127:581–592. doi:10.1083/jcb.127.3.581

Takahashi, K., S. Murakami, Y. Chikashige, H. Funabiki, O. Niwa, and M. Yanagida. 1992. A low copy number central sequence with strict symmetry and unusual chromatin structure in fission yeast centromere. *Mol. Biol. Cell*. 3:819–835.

Takahashi, K., E.S. Chen, and M. Yanagida. 2000. Requirement of Mis6 centromere connector for localizing a CENP-A-like protein in fission yeast. *Science*. 288:2215–2219. doi:10.1126/science.288.5474.2215

Talbert, P.B., and S. Henikoff. 2006. Spreading of silent chromatin: inaction at a distance. *Nat. Rev. Genet.* 7:793–803. doi:10.1038/nrg1920

Taylor, S.S., D. Hussein, Y. Wang, S. Elderkin, and C.J. Morrow. 2001. Kinetochore localisation and phosphorylation of the mitotic checkpoint components Bub1 and BubR1 are differentially regulated by spindle events in human cells. *J. Cell Sci.* 114:4385–4395.

Thiru, A., D. Nietlispach, H.R. Mott, M. Okuwaki, D. Lyon, P.R. Nielsen, M. Hirshberg, A. Verreault, N.V. Murzina, and E.D. Laue. 2004. Structural basis of HP1/PXVXL motif peptide interactions and HP1 localisation to heterochromatin. *EMBO J.* 23:489–499. doi:10.1038/sj.emboj.7600088

Toyoda, Y., and M. Yanagida. 2006. Coordinated requirements of human topo II and cohesin for metaphase centromere alignment under Mad2-dependent spindle checkpoint surveillance. *Mol. Biol. Cell*. 17:2287–2302. doi:10.1091/mbc.E05-11-1089

Van Hooser, A.A., I.I. Ouspenski, H.C. Gregson, D.A. Starr, T.J. Yen, M.L. Goldberg, K. Yokomori, W.C. Earnshaw, K.F. Sullivan, and B.R. Brinkley. 2001. Specification of kinetochore-forming chromatin by the histone H3 variant CENP-A. *J. Cell Sci.* 114:3529–3542.

Yamagishi, Y., T. Sakuno, M. Shimura, and Y. Watanabe. 2008. Heterochromatin links to centromeric protection by recruiting shugoshin. *Nature*. 455:251–255. doi:10.1038/nature07217

Yanagida, M. 2005. Basic mechanism of eukaryotic chromosome segregation. *Philos. Trans. R. Soc. Lond. B Biol. Sci.* 360:609–621. doi:10.1098/rstb.2004.1615

Published March 15, 2010

Kiyomitsu et al., http://www.jcb.org/cgi/content/full/jcb.200908096/DC1

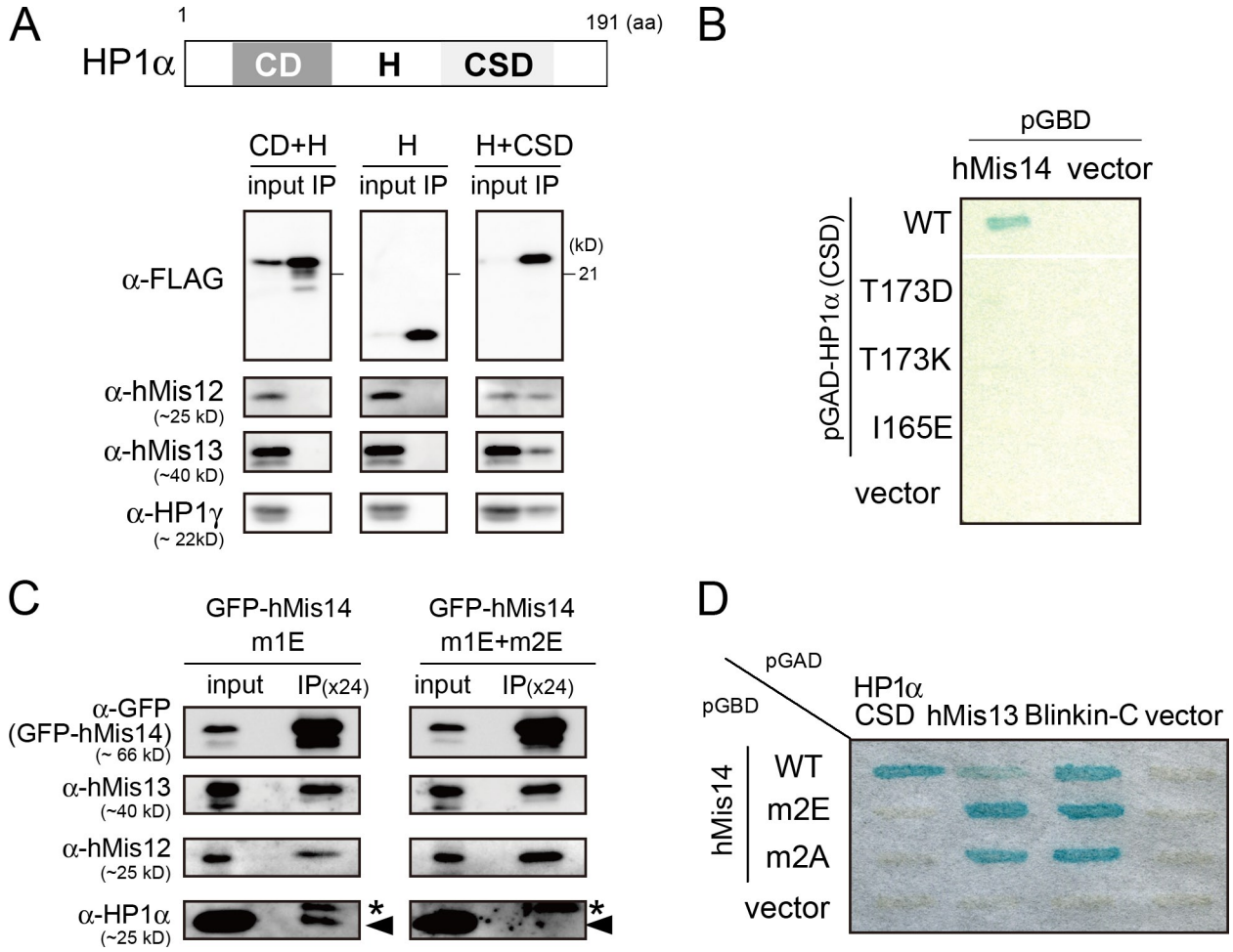

Figure S1. **The interaction between hMis14 and HP1-α.** (A) Human 293 cells were transfected with the plasmid that expressed the Flag-tagged CD and hinge (CD + H; 1–110), hinge (H; 67–110), or hinge and CSD (H + CSD; 67–191) of HP1-α. 30 h after transfection, extracts were prepared using cytoskeleton buffer and subjected to immunoprecipitation with anti-Flag antibodies. Input and immunoprecipitates (IP) were immunoblotted using antibodies against Flag, hMis12, hMis13, and HP1-γ. (B) Y2H interactions were examined between hMis14 and HP1-α CSD mutants. The white line indicates that intervening lanes have been spliced out. (C) Immunoprecipitation of GFP-tagged mutant constructs (m1E or m1E + m2E) of hMis14. Immunoblots were performed using antibodies against GFP, hMis13, hMis12, and HP1-α. The band position of HP1-α is indicated by the arrowheads. The band indicated by the asterisks is contaminating IgG. (D) Y2H interactions were examined between the hMis14 m2A mutant and HP1-α CSD, hMis13, and blinkin-C.

Published March 15, 2010

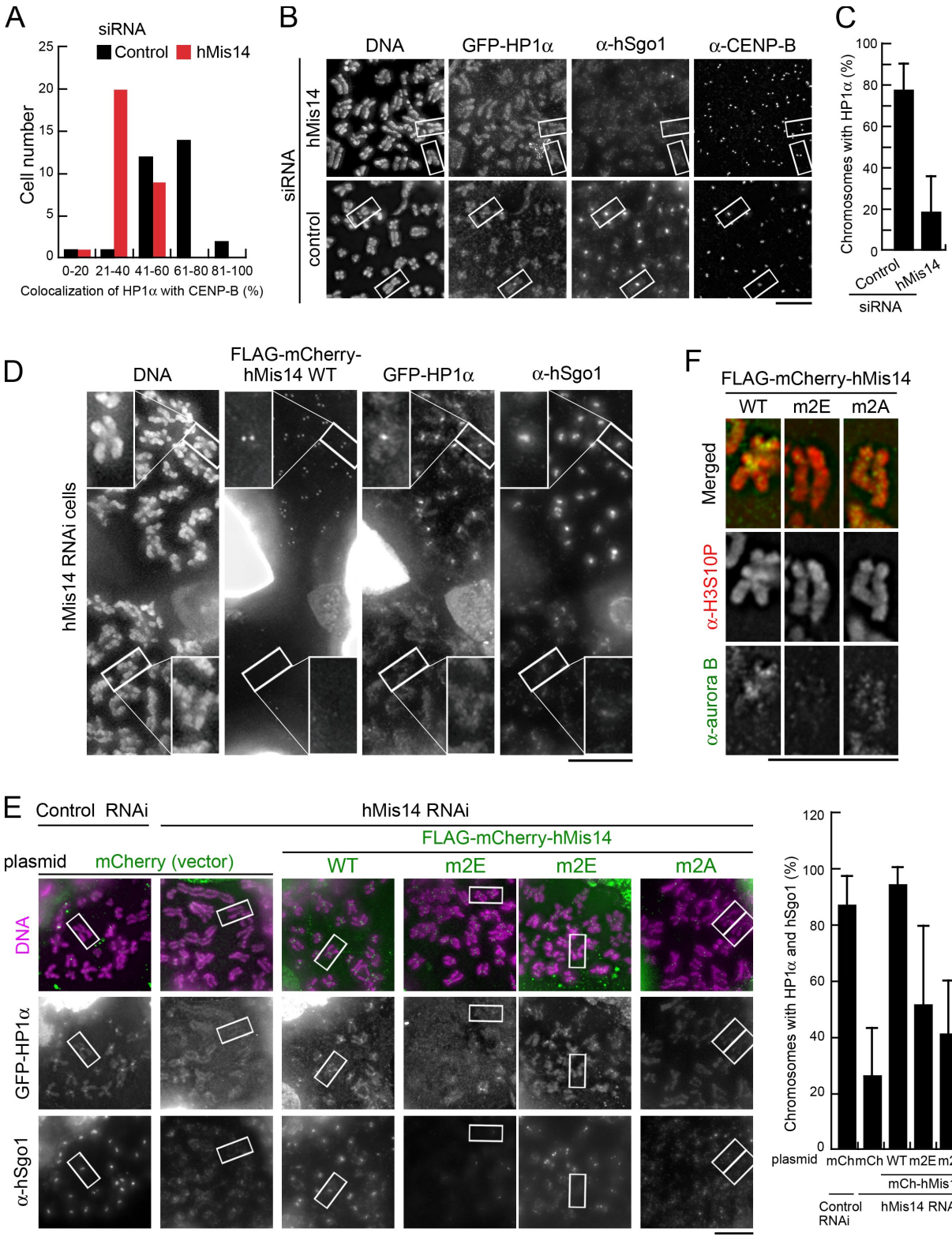

Figure S2. **hMis14 WT plasmids but not hMis14 m2E and m2A plasmids restore inner centromere enrichment of GFP–HP1-α in hMis14 RNAi cells.** (A) Frequency of GFP–HP1-α colocalization with CENP-B signals in interphase nuclei after hMis14 or control RNAi treatment (control RNAi, 60 ± 15% and *n* = 1,276; hMis14 RNAi, 35 ± 11% and *n* = 1,082). More than 1,000 centromere signals were counted from 30 interphase cells that showed neither micronuclei nor abnormal nuclei. (B) Micrographs displaying many metaphase chromosomes are shown. The chromosomes indicated with the white boxes are shown in Fig. 3 C. (C) Frequency of chromosomes with GFP–HP1-α and hSgo1 at the inner centromere (control RNAi, 77 ± 12% and *n* = 1,190; hMis14 RNAi, 19 ± 17% and *n* = 797). (D) Micrographs displaying many metaphase chromosomes are shown. Representative chromosomes indicated with white boxes are enlarged and shown in Fig. 4 B. (E) Micrographs displaying many metaphase chromosomes are shown. Representative chromosomes indicated with white boxes are shown in Fig. 4 C. The frequency of chromosomes displaying HP1-α and hSgo1 at the inner centromere in HeLa cells treated with the indicated plasmid is shown. More than 300 chromosomes from more than seven cells were measured for each sample. (C and E) Error bars represent standard deviation. mCh, mCherry. (F) The substitute experiment was performed according to the procedures depicted in Fig. 5 A using the siRNAs and cell lines indicated. Spread chromosomes were stained with anti–aurora B and anti–histone H3S10ph antibodies. Bars, 10 μm.

Published March 15, 2010

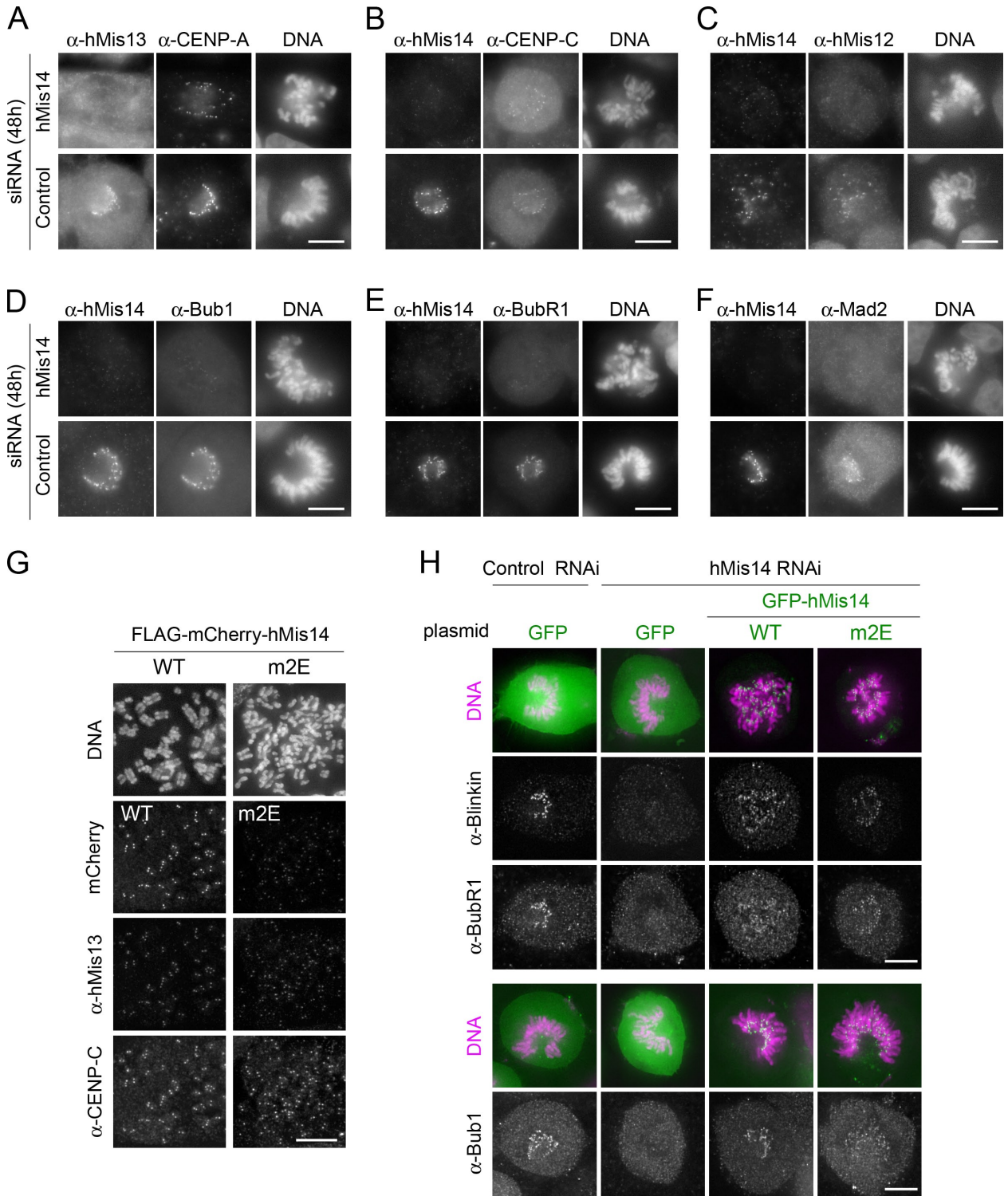

Figure S3. **hMis14-dependent localization of hMis12, blinkin, and checkpoint proteins at kinetochores.** (A–F) hMis14 (top) and control (bottom) RNAi cells were immunostained with the antibodies indicated. (G) The substitute experiment was performed according to the procedures depicted in Fig. 5 A using the siRNAs and cell lines indicated. Spread chromosomes were stained with anti-hMis13 and anti–CENP-C antibodies. (H) Cells were treated according to the procedures depicted in Fig. 4 A using the plasmids indicated and fixed and stained with Hoechst 33342 (magenta) and antibody against blinkin, Bub1, and BubR1. Cross section images were deconvolved and stacked. Bars, 10 μm.

Published March 15, 2010

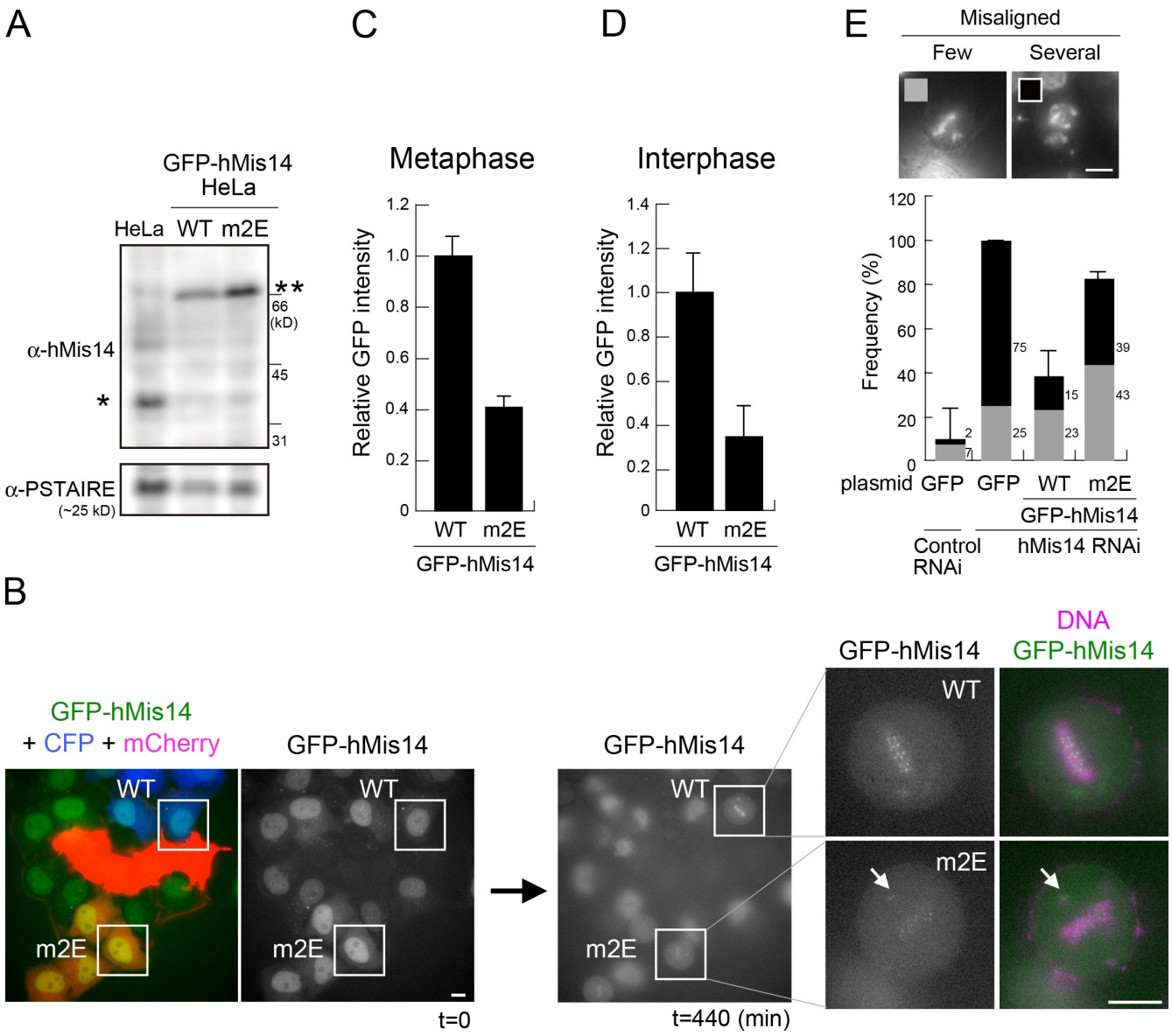

Figure S4. **HeLa cells stably expressing GFP-tagged hMis14 WT or m2E mutant were observed simultaneously.** (A) Immunoblot of hMis14 in HeLa cells stably expressing GFP-hMis14 WT or m2E mutant. The loading control was CDK1 (antibodies against PSTAIRE). Monoclonal hMis14 antibodies detected endogenous hMis14 (single asterisk) and GFP-hMis14 (double asterisk). (B) Simultaneous microscopic observation of living mitotic cells of the two HeLa cell lines expressing GFP-hMis14 WT or m2E, which were distinguished by prior transfection of plasmid carrying the CFP or mCherry gene, respectively. Arrows indicate misaligned chromosomes. (C) The GFP intensities of the hMis14 WT and m2E mutant at kinetochores in the same field were quantified as described in Materials and methods. (WT, n = 20 kinetochores from two cells; m2E, n = 40 kinetochores from four cells). (D) The GFP intensities of the centromeric signals of GFP-hMis14 WT and m2E mutant in the double thymidine–arrested cells shown in Fig. 6 D were quantified as described in Materials and methods (n = 20). Ratios of the mean intensity of hMis14 WT and the m2E mutant are shown. (E) Frequency of misaligned chromosomes in the rescue experiments after hMis14 RNAi treatment. The proportions (percentages) of cells containing a few or several misaligned chromosomes were measured during mitotic progression in the videos. To take several videos, we performed each rescue experiment twice, and the total number of the cells observed is shown in Fig. 7 C. (C–E) Error bars represent standard deviation. Bars, 10 μm.

Published March 15, 2010

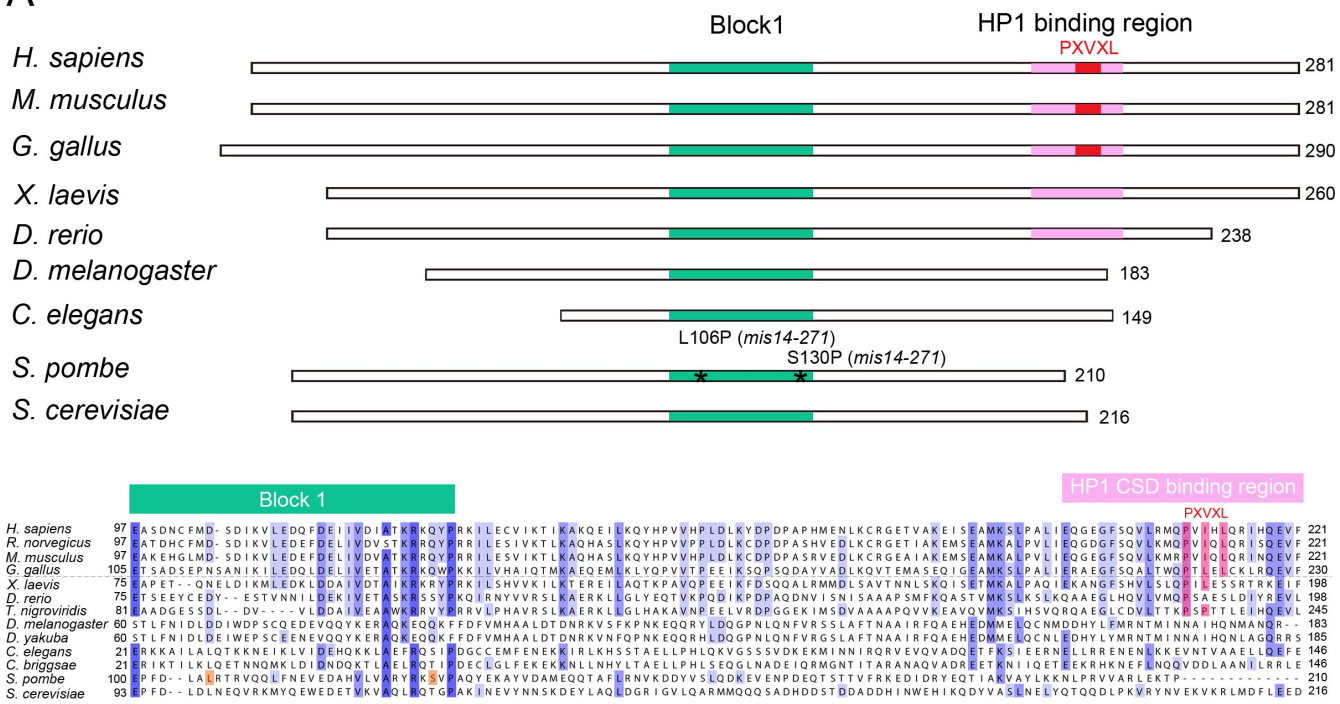

(Block 1; Meraldi et al., 2006; Przewloka et al., 2007)

(*S. pombe mis14* mutants; Hayashi et al., 2004)

Figure S5. **Amino acid sequence alignment of the Mis14 family of proteins.** (A) Amino acid sequence alignment of the Mis14 family of proteins. Amino acid sequences of putative Mis14 family members in *Homo sapiens* (NP_056286), *Rattus norvegicus* (NP_001102553), *Mus musculus* (NP_941056), *Gallus gallus* (NP_001038111), *Xenopus laevis* (ACV87358), *Danio rerio* (NP_001020692), *Tetraodon nigroviridis* (CAF89539), *Drosophila melanogaster* (NP_572729), *Drosophila yakuba* (XP_002100850), *Caenorhabditis elegans* (NP_498495), *Caenorhabditis briggsae* (XP_002641863), *S. pombe* (NP_594061), and *S. cerevisiae* (NP_015091) are aligned. Identical residues present in >80% of the organisms are boxed in dark purple, and similar ones present in >60% or >40% are boxed in purple or light purple, respectively. HP1-binding PXVXL motifs are shown in red. Block 1 is cited from previous studies (Meraldi et al., 2006; Przewloka et al., 2007). Amino acids changed in *S. pombe mis14* mutants (Hayashi et al., 2004) are boxed in orange. (B) Amino acid sequences of TIF1-α family members in *H. sapiens* (NP_056989), *M. musculus* (NP_659542), *Taeniopygia guttata* (XP_002191494.1), *G. gallus* (XP_416340), and *D. rerio* (NP_001002870.2). (A and B) Accession numbers are from the NCBI Protein database.

Published March 15, 2010

References

Hayashi, T., Y. Fujita, O. Iwasaki, Y. Adachi, K. Takahashi, and M. Yanagida. 2004. Mis16 and Mis18 are required for CENP-A loading and histone deacetylation at centromeres. *Cell*. 118:715–729. doi:10.1016/j.cell.2004.09.002

Meraldi, P., A.D. McAinsh, E. Rheinbay, and P.K. Sorger. 2006. Phylogenetic and structural analysis of centromeric DNA and kinetochore proteins. *Genome Biol.* 7:R23. doi:10.1186/gb-2006-7-3-r23

Przewloka, M.R., W. Zhang, P. Costa, V. Archambault, P.P. D'Avino, K.S. Lilley, E.D. Laue, A.D. McAinsh, and D.M. Glover. 2007. Molecular analysis of core kinetochore composition and assembly in *Drosophila melanogaster*. *PLoS One*. 2:e478. doi:10.1371/journal.pone.0000478